Année 2010

EU4M : EUropean Master in Mechatronics
and MicroMechatronics Systems

Mémoire de stage master

Domaine : Sciences – Technologies – Santé

Mention : Sciences Pour l'Ingénieur

Spécialité

Mécanique – Mécatronique – Microsystèmes et Ingénierie

Relations internationales ENSMM

Modélisation et identification d'un robot à câbles

Tien Thanh NGUYEN

Equipe Automatique Vision et Robotique
LSIIT - UMR 7005
Pôle API
Bd Sébastien Brant
BP 10413
67412 Illkirch CEDEX FRANCE

Remerciements

Je tiens à remercier Madame le Professeur Nadine Le Fort-Piat et Monsieur le Professeur Claude Roche de mavoir accueillie au Master 2 à Besançon, de mavoir aidé toutes mes difficultés dans mes études.

Ma gratitude va également à Monsieur le Professeur Edouard Laroche qui a dirigé mon travail. Ses conseils et ses commentaires précieux m'ont permis de surmonter mes difficultés et de progresser dans mes études.

Je voudrais également remercier Monsieur le Professeur Jacques Gangloff, qui par son expérience et son enthousiasme, ma aussi donné beaucoup de propositions tout au long de ce stage.

Je nomettrai pas de remercier Loic Cuivillon et tous les membres de l'équipe Automatique, Vision et Robotique du LSIIT pour leur accueil, leur sympathie ainsi que leurs idées constructives.

Et enfin, je voudrais adresser mes remerciements à ma famille pour mavoir encouragé beaucoup dans mes mes études.

Résumé

Le stage que nous allons présenter ici est le résultat de six mois d'études à Strasbourg, France. Ce travail a été fait à l'équipe Automatique, Vision et Robotique (eAVR) du Laboratoire des Sciences de l'Image, de l'Informatique et de la Télédétection.

L'objectif principal de cette stage est de développer un modèle dynamique pour le robot INCA et d'estimer les paramètres de l'expérience des données. Le robot INCA est conçu et fabriqué par la société Haption. Le mécanique de robot INCA se compose d'une plate-forme mobile et huit câbles. La plate-forme mobile est entraîné par les huit câbles. Chaque câble est actionné par Cable Driving Unit (CDU). Le CDU compris un moteur à courant continu et un système de ressort supplémentaire et est positionnés sur un cadre de base. Pour des raisons d'origine, il s'agit d'un 6 degrés de liberté dispositif haptique, spécialement conçus pour travailler en réalité virtuelle. Pour des raisons de robotique, en fonction de ses propriétés mécaniques, le robot INCA est dans la classe de robots parallèles entraînés par câble. Grace à les avantages des deux structures parallèles et de légèreté de conduite câbles, robot INCA possède de nombreuses caractéristiques importantes, telles que: la capacité de charge élevée, le mouvement à grande vitesse, grand espace de travail, mais faible consommation d'énergie, faible moment d'inertie, peu d'interférences mécaniques, structure simple et légère de poids. Pour cette raison, les travaux qui sont contribué à l'étude de la modélisation et l'identification du robot INCA, sont volontairement demandé.

De manière générale, le principal problème de la modélisation est de construire un modèle qui se comporte, aussi semblables que cela est possible, comme le système réel. Cependant, nous ne pouvons pas avoir une connaissance complète du système, parce qu'il est souvent difficile de connaître toutes les relations physiques que le système a l'intérieur. Ainsi, il est important de se concentrer sur les principales caractéristiques du système et de ne pas tenir compte des caractéristiques mineures. Dans ce cas, la modélisation du robot INCA est basée sur des études approfondies de son architecture mécanique et son comportement dynamique, et aussi les travaux de recherche connexes. Ainsi, plusieurs approches sont considérées comme de choisir l'approche la plus efficace pour modéliser le robot INCA. Dans cette approche, une liste d'hypothèses est proposé, le modèle est construit selon la procédure d'analyse de robot.

Tout d'abord, la cinématique du robot INCA est étudiée par la méthode géométrique de la même manière qu'avec les robots parallèles rigides. Ensuite, la dynamique de chaque bloc constituant le robot INCA est analysé séparément. Dans cette étude, le comportement dynamique du câble dans le robot INCA est considérée comme la principale caractéristique du système dynamique, et est soigneusement analysé. Le modèle dynamique du câble est proposé. Dans ce modèle, l'élasticité et le comportement d'amortissement du câble qui dépendent de l'action du rouleau, sont comptabilisés. Une méthode pour

déterminer les tensions internes des câbles est présenté. Toutefois, en raison de la faible incidence de la masse de câbles sur la dynamique du système, la dynamique de la masses de câbles sont négligés. Les masses des câbles ne sont comptabilisés dans le moment d'inertie attachés aux moteurs à courant continu. La dynamique de la plate-forme mobile est analysée par les équations dynamiques de 6 degrés de liberté de corps rigide, avec les forces actionnés sont les tensions des câbles. De la même façon, la dynamique de l'actionneur est déterminée en fonction de l'équation de la loi de Newton écrite pour le moteur à courant continu, avec les charges proviennent des tensions des câbles. La combinaison de l'équation dynamique de 3 blocs, les équations de la dynamique de l'ensemble du système sont écrites comme un ensemble de fonctions d'état-espace, qui est mis en uvre dans une S-fonction de Matlab. Pour rendre visible la simulation et à utiliser dans le contrôle visuel du robot INCA, un programme qui anime robot INCA en matière de simulation a été développé.

Après avoir construit le modèle dynamique, l'une des approches pour étudier le système est mesurer tous les paramètres physiques à l'intérieur des équations dynamiques. Cependant, il ne se passe pas si souvent d'avoir tous les paramètres nécessaires de ces relations, nous devons donc les trouver en quelque sorte. Voici la théorie de *l'identification paramétrique* donne nous aider à nous avec ses méthodes. Ce sujet est divisé en deux branches différentes: *Blackbox Identification* et *Greybox Identification*. Dans cette étude, le modèle dynamique du robot INCA qui a été étudiée à fond, est utilisé comme un modèle non linéaire greybox. Il est écrit comme un ensemble de fonctions non linéaires où les paramètres sont inconnus:

$$\begin{aligned} \dot{x}(t) &= f(t, x(t), \wp, u(t)) \\ y(t) &= h(t, x(t), \wp, u(t)) + e(t) \end{aligned} \tag{1}$$

où f et h sont des fonctions non linéaires. $x(t)$ est le vecteur d'état, $u(t)$ et $y(t)$ sont signaux d'entrée et de sortie. $e(t)$ est un signal de bruit, et t désigne le temps. Enfin $\wp$ est le vecteur des paramètres inconnus. Un critère de distance est conçu entre la sortie mesurée vecteur y et le vecteur de sortie estimée $\hat{y} = h(x, u, \wp)$ selon $\wp$. Le vecteur paramètre est estimé par la minimisation d'une fonction scalaire par la méthode de programmation non linéaire. Dans ce cas, l'ensemble de la fonction non linéaire décrit le modèle greybox est obtenu à partir des équations de l'espace d'état dans le modèle dynamique. Les signaux d'entrée et de sortie sont acquis à partir de l'expérience sur le robot INCA. La méthode utilisée pour minimiser le critère est la méthode itérative de minimisation d'erreur de prédiction, qui est disponible dans System Identification Toolbox. Néanmoins, l'identification donne un modèle précis aux fréquences où le signal d'entrée contient beaucoup d'énergie. Par conséquent, le choix du signal d'entrée qui a une bonne excitation est une condition importante pour l'identification. En outre, le *Identifiabilité* du robot INCA est également nécessaire pour être étudiée.

En théorie, un système est identifiable si il existe une procédure qui amène à une valeur unique du vecteur paramètre $\wp$ et à un modèle estimé le même comportement du système réel. Un autre aspect de l'identification est le *Sensibilité* de chaque paramètre. Le *Sensibilité* étudie les effets des variations des paramètres sur la valeur des critères de la fonction. Pour l'analyse de ces aspects dans l'identification du robot INCA, et obtenir la procédure la plus efficace pour l'identification de l'INCA robot, plusieurs essais d'identification avec des données simulées qui ont été acquis de la simulation, sont traitées. Les facteurs suivants: nombre de paramètres estimés, les valeurs initiales qui sont prévues pour l'identification et le bruit, qui ont des effets sur le résultat d'identification sont analysés. Selon le résultat d'analyse, une procédure d'identification de robot INCA est proposé. Le modèle non linéaire greybox est identifié avec les données expérimentales qui sont acquis à partir du robot. Le modèle estimé est également validé, il peut être utilisé comme référence pour l'identification LPV, ou utilisés pour la prédiction qui aide dans la controleur.

Contents

List of Abbreviations

$\dot{\mathbf{v}}_{bi}$	acceleration of the ball point B_i , expressed in the fixed frame
$\dot{d}_i = \dot{d}$	rate of length cable change
ε	strain or relative elongation of cable
Γ, Γ_m, Γ_l	torque applied, motor torque and torque load
ω_p	angular velocity of moving platform
ϕ, θ, ψ	roll, pitch and yaw angles of moving platform coordinate related to fixed base
ϕ_i, θ_i	2 Euler angles describe orientation of each cable related to fixed base
σ	tensile stress of cable
$\mathbf{a}_i$	position vector of $\mathbf{A}_i$ with respect to the fixed frame
$\mathbf{b}_i$	vector ${}^B\mathbf{b}_i$ expressed in the fixed frame
$\mathbf{s}_i$	unit vector pointing from $\mathbf{A}_i$ to $\mathbf{B}_i$
$\mathbf{v}_{bi}$	velocity of the ball point B_i in fixed base coordinate
φ	rotation angle of motor
${}^AR_B$	rotation matrix of moving platform relative to fixed base
${}^B\mathbf{b}_i$	position vector of $\mathbf{B}_i$ with respect to the moving frame
${}^i\dot{\omega}_i$	angular acceleration of the cable i
${}^i\dot{\mathbf{v}}_{bi}$	acceleration of the ball point B_i , expressed in cable frame
${}^i\omega_i$	angular velocity of cable in cable frame

$^i\mathbf{v}_{bi}$ velocity of B_i expressed in the i cable frame

^iR_B rotation matrix of the ith cable coordinate to fixed base

b damping coefficient of cable

d_0 no-load length of cable

d_i the length of cable i

E Young modulus of cable material

F_p applied force to MP in moving platform frame

G_p external disturbance forces

J_m, b_m, K_t moment inertia, damping ratio and torque constant of motor

k_s spring constant of additional spring

m and I body mass and inertia tensor of MP with respect to origin point P

M_p applied moment to MP in moving platform frame respect to origin point P

$O(x, y, z)$ coordinate frame attracted to fixed base A

$P(u, v, w)$ moving coordinate frame located at center of mass P of moving platform B

R Radius of motor roller attracted to cable

R_s Radius of motor roller attracted to additional spring

S cross section area of the cable element

s_{ix}, s_{iy}, s_{iz} x, y, and z components of $\mathbf{s}_i$

T tension of cable within elastic and damping behaviour

T_d forces in the cable generated by damping

T_e tension within elastic behaviour of cable

w angular velocity of motor

List of Figures

List of Tables

Chapter 1

Introduction

Contents

1.1 Cable-Driven Parallel Robot

Cable-driven parallel robots (CDPRs) are a type of parallel robotic manipulator which utilize multiple cables to actuate an end-effector within a defined workspace. Benefiting from the advantages of both parallel kinematics structures and light-weight driving cables, a CDPR has the following significant features:

- Simple and light-weight mechanical structure
- High loading capacity and low energy consumption
- Low moment of inertia and high speed motion
- Large workspace and few mechanical interferences

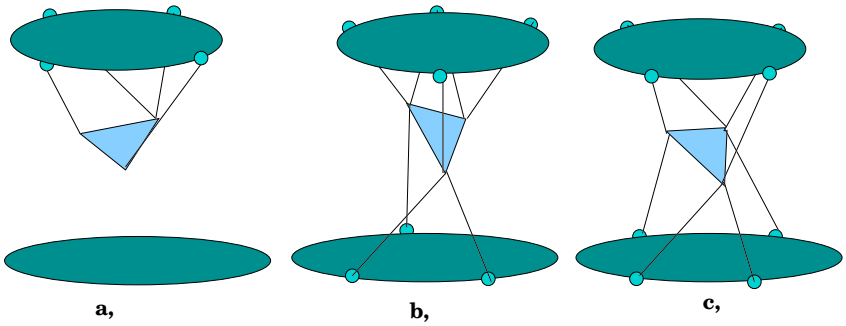

Figure 1.1: *Cable-driven parallel robots: a: incompletely restrained CDPR, b: completely restrained CDPR, c: redundantly restrained CDPR*

These advantages make the CDPRs promising alternatives of the rigid-link manipulators in many industrial applications, such as load lifting and positioning, such as robot crane [8], camera positioning for sport events [5], aircraft testing [12], haptic devices [17], and robotic rehabilitations.
Based on the number of driven cables (m) and the number of degrees of freedom (n), the CDPRs were classified into three categories:

- incompletely restrained CDPR ($m < n + 1$)
- completely restrained CDPR ($m = n + 1$)
- redundantly restrained CDPR ($m > n + 1$)

For an incompletely restrained CDPR, additional constraints like gravity should be employed in order to obtain deterministic motions of the moving platform [1]. Consequently, only certain degrees of freedom of the moving platform can be realized. The completely restrained CDPR is a particular class of the CDPRs whereby all possible degrees of freedom can be realized by using a minimum number of driven cables. For a redundantly restrained CDPR, there exists actuation redundancy. Although redundant actuation is an effective approach for singularity avoidance [15], sophisticated dynamic control schemes need to be investigated.
However, cables have one special property - they carry loads in tension but not in compression. Due to this feature, well known results in robotics for trajectory planning and control are not directly applicable to cable robots but must be modified to reflect the constraints of positive cable tensions.

1.2 State of the Art

A significant amount of work has been done in both the areas of Cable Driven Parallel Robots and identification of robotic system. In the area of modelling CDPRs, the

main focus is in modelling cable with elasticity and mass. Supporting cables in cable-suspended manipulator can be modelled with springs and dampers [18]. Kozak and et al. analysed the effect of cable mass in the static of incompletely restrained CDPR [11]. Inextensible cable simplification was applied. The results showed that cable sag can have a large effect on both the inverse kinematics and the stiffness of a CDPR. A method for compensating the deflections caused by cable self-weights is described in Jeong et al. [9]. Jeong determined the nonlinear equations of the forward kinematics from the geometric configuration of the mechanism. In the work of Korayem et al. [10], A 3D geometric model of the cable that include sag and elongation is fully accounted for work space analysis of incompletely restrained CDPR. The dynamics and control of planar redundantly restrained CDPRs are studied by Williams et al. [6] and Pham et al. [15]. However, there has been not much research in modelling redundant CDPRs with 6 degrees of freedom, and in the phenomenon of cable elasticity depending on the roller's action.

System identification in robotics is a vast research area. Many works focus on identification for the industrial robots containing flexibilities [14] and friction [7]. Because of its advantages, the grey-box identification has now been reasonably well accepted as a paradigm for how to address the practical problems in identifying physical processes. Several tools are designed for grey-box identification, such as MoCaVa [2], System Identification Toolbox of Matlab [13] and IdKit [3].

1.3 INCA robot

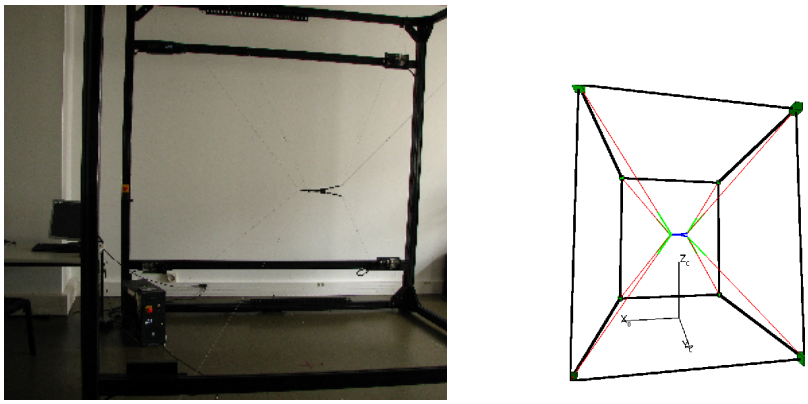

Figure 1.2: *Photo of INCA robot in EAVR and in animation*

The INCA 6D is a haptic device with very large workspace offering force-feedback on all 6 degrees of freedom, especially suited for immerse environments. It has been

designed for virtual assembly/disassembly operations in CAD and Virtual Reality applications. The INCA 6D cable-driven haptic device is based on the SPIDAR^{TM} of Professor Sato [16] and is designed and manufactured by Haption company. The INCA 6D is specifically designed for work in Virtual Reality environments. Thanks to its large workspace and its high forces, it enables a scale one interaction with digital models coming from CAD. Data-sheet [4] and information of INCA 6D haptic device can be found in Haption's website [1].
As a robot, INCA 6D is a redundantly restrained cable driven parallel robot, with 8 cables, actuated by 8 Cable Driving Units (CDU), drives a moving platform on all 6 degrees of freedom (3 translations and 3 rotations). Figure 1.2 represents a picture of INCA 6D robot. Mechanical architecture of INCA 6D will be described in next sections.

1.4 Objectives, Methodology and Structure of the thesis

1.4.1 Objectives

The main objective of this thesis is to develop the dynamic models of the INCA robot from the laws of physics and to estimate their parameters from the experimental data.

1.4.2 Methodology

Firstly, to study the kinematic analysis of such structures in detail, geometry method is used, a vector-loop equation is written for each loop. Then, dynamic behaviour of the robot is analysed using the well-known Newton-Euler formulation. A simplified elastic model of cable is proposed to determine the cable dynamics. For this purpose, it is assumed that the effect of cable mass on dynamics moving platform is negligible but the cable elasticity and damping effect is accounted and depend on the action of the roller. Combined with the dynamics of the cables, the dynamic of actuators and the moving platform are introduced, thereby the dynamic model of the whole system is written as a non-linear state-space function. To identify the INCA robot, a non-linear grey-box model of the robot is constructed based on the the state state-space function written above:

$$\begin{aligned} \dot{x}(t) &= f(t, x(t), \wp, u(t)) \\ y(t) &= h(t, x(t), \wp, u(t)) + e(t) \end{aligned} \tag{1.1}$$

where f and h are nonlinear functions. $x(t)$ is the state vector, $u(t)$ and $y(t)$ are input and output signals, $e(t)$ is disturbance signal, and t denotes time. Finally $\wp$ is the vector of unknown parameters. A distance criterion is designed between the measured output vector y and the estimated output vector $\hat{y} = h(x, u, \wp)$ depending on $\wp$. The parameter vector is estimated by minimizing a scalar function through non-linear programming

[1] www.haption.com/site/eng/images/pdf_download/Datasheet_Inca.pdf

method. In this thesis, the iterative prediction-error minimization method introduced in System Identification Toolbox of Matlab, is used. To improve the identification results, several identification trials are processed with the simulated data. All of the factors which are able to affect the identification result, are analysed. Finally one procedure for identification of the INCA robot is proposed, the estimated model is represented.

1.4.3 Structure of the thesis

This thesis is divided in three chapters: chapter I introduces the INCA robot and its robot group, a brief introduction to related works in modelling Cable Driven Parallel Robots and in identification of robot system is represented. Chapter II deals with the topic of modelling kinematics and dynamics of the INCA robot. A dynamic model of the INCA robot is contributed. Chapter III deals with estimation of the parameters and initial states of INCA robot from the grey-box model that was introduced in chapter II. Finally, in the last chapter, there are summarizes and conclusions about this work.

Chapter 2

Modelling of the INCA robot

Contents

INCA robot is a redundantly restrained cable driven parallel robot with 8 driven cables and 6 degrees of freedom. Kinematics of INCA robot can be analysed as kinematics of a rigid parallel robot. Dynamics of INCA robot is separately analysed in 3 parts: the 8 elastic cables, the moving platform and the 8 actuators. Figure 2.1 represents the block diagram of INCA robot dynamics: In this section, firstly the mechanic structure of the INCA robot is introduced, then the kinematics of the INCA robot is investigated

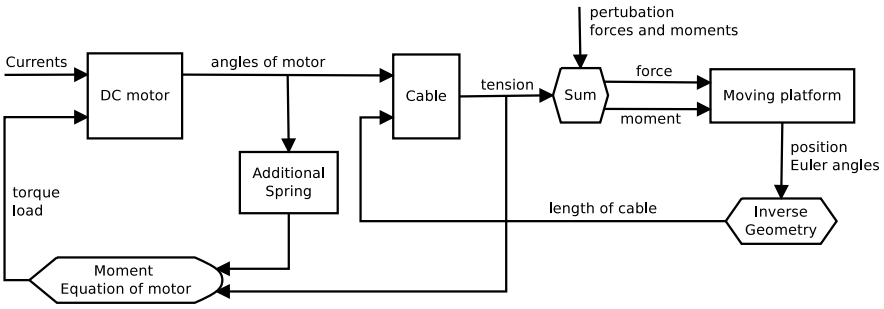

Figure 2.1: *Block diagram of INCA robot dynamics*

in term of parallel robot's kinematics. Finally, a dynamic model of the INCA robot, including dynamics of cables, the moving platform and motors, is represented in the last section. List of the assumptions used in the analysis of the INCA robot is introduced below:

- In the kinematics analysis, we assume that cable mass and its elasticity are negligible. Therefore, there is no phenomenon of the sag of cable which effects on the kinematics of the robot. Hence, the analysis method for the rigid parallel robot can be applied to investigate the kinematics of the INCA robot.
- The radius of the pulleys are negligible. Thus it has no effect on the kinematics of the robot. The free rotational pulley, which will mentioned in the next section, is considered as a ball joint.
- The cable mass is also neglected in the dynamics analysis of the cable. However, the mass of cable is accounted in the moment of inertia of the motor.

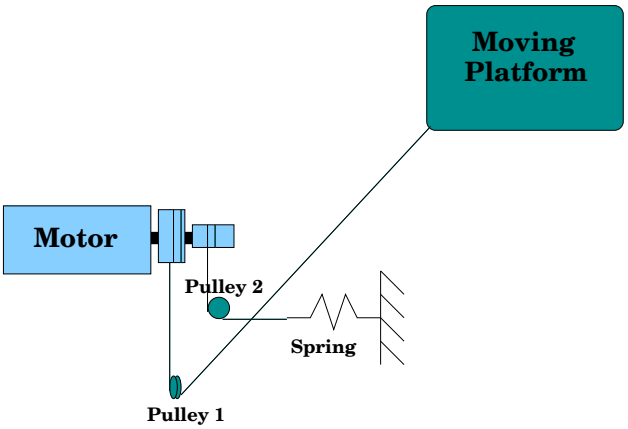

Figure 2.2: *Cable Driving Unit (CDU)*

2.1 Mechanic system architecture

The INCA robot's mechanics consists of a moving platform and eight cables. Each cable is driven by Cable Driving Unit (CDU) including a DC motor and an additional spring system. Each motor is used to control the length of exactly one cable whose route is from the actuator to the moving platform via a pulley. The additional spring system attached at another drum of the motor. The 8 additional spring systems are used to produce initial tensions in cables, keep the moving platform in balanced position when the control is off or in case of electric supply failure and help reducing load for motors. Position and number of motors is shown in Figure 2.3, that are provided by manufacturer Haption. According to datasheet from Haption, mechanic architecture of

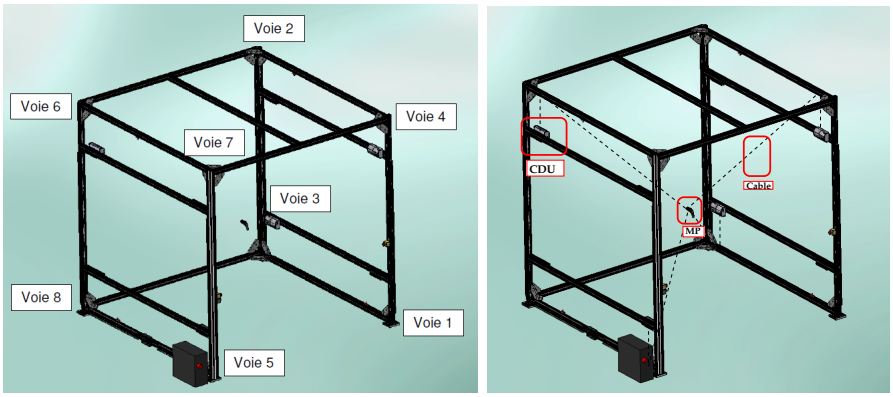

Figure 2.3: *Scheme of INCA robot with number of motor*

the INCA robot includes these following elements.

- engine blocks
- deviation systems for cable
- balancing system
- moving platform or end effector
- structure of the based frame

Each element will be introduced separately in the following subsections.

2.1.1 Engine blocks

Figure 2.4 represents a open engine block of the INCA robot and its components. The main components of the engine block are a Maxon graphite brushes DC motor and an electro-optical incremental encoder. The mechanical coupling is used to transfer

load from the motor to the 2 rollers (or drums). Two rollers have the same axle-axis but different radius, one roller connects to the cable of balancing system, and other connects to the cable driving the moving platform. A potentiometer with gear and conveyor is included in the engine block to control motor speed and to measure the absolute rotation of the motor.

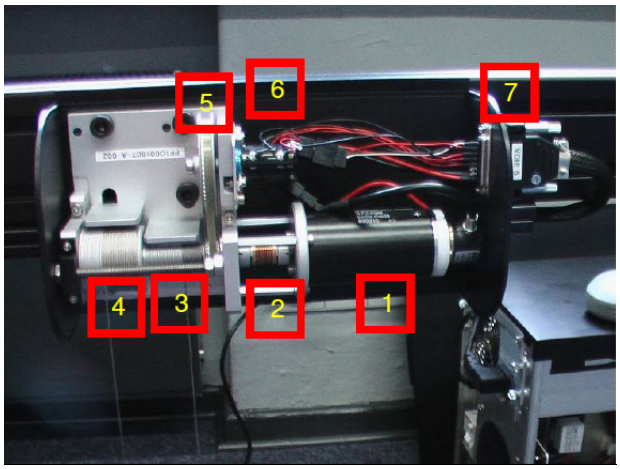

Figure 2.4: *Engine block of INCA robot:*
1. DC motor and electro-optical encoder
2. Mechanical coupling
3. Drum for the cable of the balancing system
4. Drum for the cable driving the moving platform
5. Gear and conveyor for potentiometer
6. Potentiometer
7. Electrical connection

2.1.2 Deviation systems for cable

Figure 2.5.a represents the deviation systems for the cables, positioned under each engine block. It is composed of two pulleys:

1. one fixed axis pulley to deviate the cable of balancing system

2. one free rotational pulley to bypass cable to moving platform. A scheme of a free rotational pulley is shown in Figure 2.5.b. It has 2 degrees of freedom, and is considered as a ball joint. It allows cable to rotate in two axis but cannot rotate about its longitudinal axis.

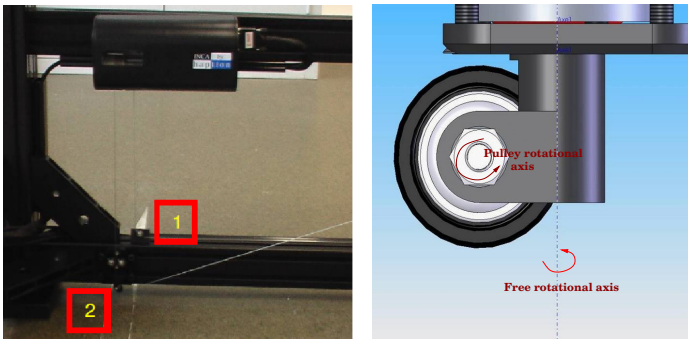

(a) *Deviation systems for cables* **(b)** *Free rotational pulley*

Figure 2.5: *Deviation systems for cable and free rotational pulley: 1. fixed axis pulley, 2. Free rotational pulley*

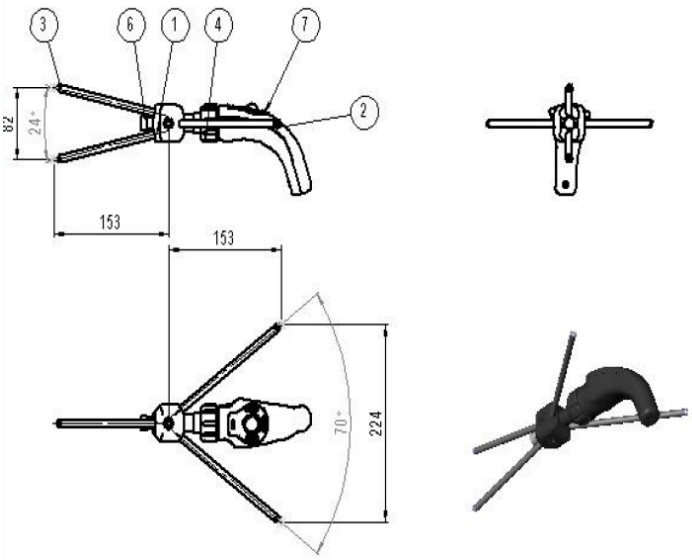

Figure 2.6: *Scheme of moving platform includes Cobra handle*

2.1.3 Moving platform

In this project, the moving platform of INCA robot is mentioned as a end-effector of a manipulator. It is a rigid body with 4 connectors attracted to 8 cables, shown in Figure 2.6. However, the moving platform can be replaced in order to comfort with application of INCA robot.

2.1.4 Balancing system

As can be seen in Figure 2.2, each cable in the pulley number 2 of a motor is connected to a tension spring (4 springs for INCA 3D or 8 springs for INCA 6D). This spring exerts a tension on the cable to help reducing load for motors. Moreover, when the voltage is out of INCA, the cables are always tense, keep moving platform in a balancing position.

2.1.5 Structure of the based frame

For cable driven parallel robot, the whole workspace is limited by the based frame. In general case, the based frame can be modified based on the fixed positions of CDUs. In INCA robot, the based frame is an aluminium frame, which is fixed to the ground. All the CDUs have fixed positions in the based frame. Hence, all the ground reaction forces produced while INCA robot is working, have produce effects on the based frame and make it vibrate. Therefore, the structure of the based frame must be strong enough to reduce the vibration. On the structure the two emergent stop-buttons and a power switch are positioned.

2.2 Kinematics of the INCA robot

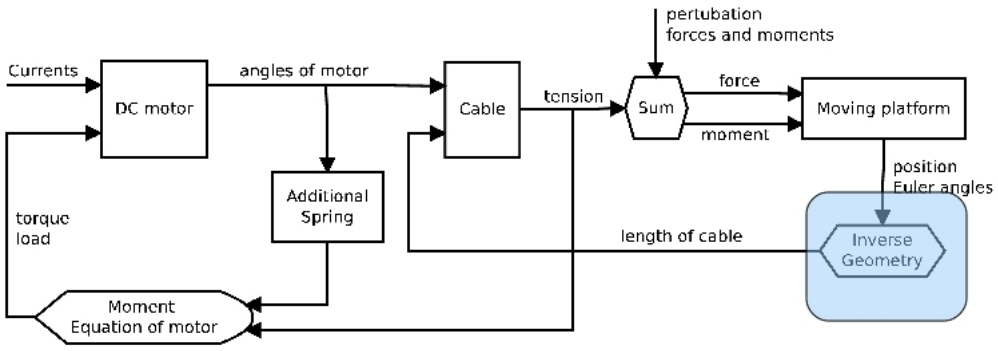

Figure 2.7: *Block diagram of dynamic model of the INCA robot: Kinematics*

In this section, the kinematics of the INCA robot is investigated by the geometry method, which is commonly used for analysing kinematics of parallel robot. In the block diagram, only the inverse geometry is included, however, all the kinematics of the INCA robot: geometric, velocity, acceleration are analysed for the purpose of further research.

For the purpose of analysis, the following coordinate frames are defined (see Figure (2.8)):

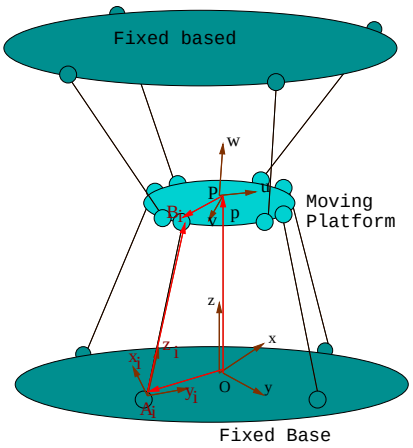

Figure 2.8: *Schematic diagram of INCA robot*

- the coordinate frame of based frame (O, x, y, z) is attached to the center of ground floor of the fixed base A. It is considered as the ground reference coordinate of all the movement in INCA robot.
- the coordinate frame (P, u, v, w), attached to the moving platform, is located at the center of mass P of the moving platform B.
- the coordinate frame of cable (A_i, x_i, y_i, z_i) is attracted to the joint A_i of based frame and z_i is pointing in the cable direction towards B_i.

We use the common notation used in robotics kinematic analysis of INCA robot: ${}^aX_b$ where X_b is position vector or velocity vector or acceleration vector or rotation matrix of point or coordinate b. ${}^aX_b$ denotes the X_b expressed in the coordinate a. We use A to denote the based frame, B to denote the moving platform frame and i to denote the frame attracted to the cable ith frame.

The pose of the moving platform can be described by a position vector $\mathbf{p}$ of the centroid P and a rotation matrix ${}^AR_B$. Let the rotation matrix be defined by the roll, pitch, and yaw angles, namely, a rotation of ϕ about the fixed x axis, resulting in an (u', v', w') system, followed by a rotation of θ about the fixed y axis, resulting in an (u'', v'', w'') system, and a rotation of ψ about the fixed z axis, resulting in an (u, v, w) system. The rotation matrix of the moving platform relative to the fixed base is given by:

$$ {}^AR_B = \mathrm{Rot}(z, \psi)\,\mathrm{Rot}(y, \theta)\,\mathrm{Rot}(x, \phi)^1 \tag{2.1}$$

[1] $Rot(x,\phi) = \begin{bmatrix} 1 & 0 & 0 \\ 0 & \mathrm{c}\phi & -\mathrm{s}\phi \\ 0 & \mathrm{s}\phi & \mathrm{c}\phi \end{bmatrix}$ $Rot(y,\theta) = \begin{bmatrix} \mathrm{c}\theta & 0 & \mathrm{s}\theta \\ 0 & 1 & 0 \\ -\mathrm{s}\theta & 0 & \mathrm{c}\theta \end{bmatrix}$ $Rot(z,\psi) = \begin{bmatrix} \mathrm{c}\psi & -\mathrm{s}\psi & 0 \\ \mathrm{s}\psi & \mathrm{c}\psi & 0 \\ 0 & 0 & 1 \end{bmatrix}$
where $s\phi$ denotes sine of angle ϕ while $c\phi$ denotes cosine of angle ϕ

The angular velocity ω_p of the moving platform is written in term of the rate of change of the Euler angles and the body-fixed **u**, **v** and **w** unit vector, is

$$\omega_p = \dot{\phi}\mathbf{u} + \dot{\theta}\mathbf{v} + \dot{\psi}\mathbf{w} \tag{2.2}$$

The relationship between the body-fixed angular velocity vector, ω_p, and the rate of change of the Euler angles, $[\dot{\phi}\ \dot{\theta}\ \dot{\psi}]^T$, can be determined by resolving the Euler rates into the body-fixed coordinate frame.

$$\omega_p = \begin{bmatrix} \dot{\phi} \\ 0 \\ 0 \end{bmatrix} + \mathrm{Rot}(x,\phi) \begin{bmatrix} 0 \\ \dot{\theta} \\ 0 \end{bmatrix} + \mathrm{Rot}(x,\phi)\mathrm{Rot}(y,\theta) \begin{bmatrix} 0 \\ 0 \\ \dot{\psi} \end{bmatrix} \tag{2.3}$$

This equation can be written as:

$$\omega_p = J^{-1} \begin{bmatrix} \dot{\phi} \\ \dot{\theta} \\ \dot{\psi} \end{bmatrix} \tag{2.4}$$

Inverting J then gives the required relationship to determine the Euler rate vector.

$$\begin{bmatrix} \dot{\phi} \\ \dot{\theta} \\ \dot{\psi} \end{bmatrix} = J\,\omega_p = \begin{bmatrix} 1 & (\sin\phi\tan\theta) & (\cos\phi\tan\theta) \\ 0 & \sin\phi & -\sin\phi \\ 0 & \frac{\sin\phi}{\cos\theta} & \frac{\cos\phi}{\cos\theta} \end{bmatrix} \omega_p \tag{2.5}$$

The rotation matrix and angular velocity of the moving platform have been computed. Kinematics of the INCA robot: the geometric, velocity and acceleration analysis are investigated based on the geometry method in the next subsections.

2.2.1 Geometric Analysis

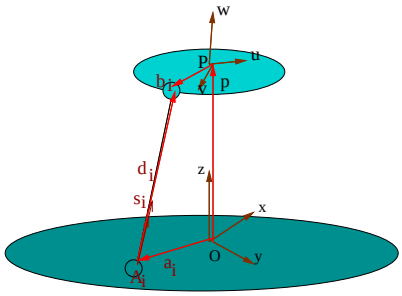

Figure 2.9: *Vector diagram of the ith kinematic chain.*

As shown in Figure 2.9, the closed-loop position vector equation associated to the ith kinematic chain can be written as:

$$\mathbf{a}_i + d_i\mathbf{s}_i = \mathbf{p} + \mathbf{b}_i \tag{2.6}$$

where $\mathbf{a}_i$ denotes the coordinate of $\mathbf{A}_i$ ($\overrightarrow{OA_i}$) expressed in the fixed frame, ${}^B\mathbf{b}_i$ denotes the coordinate of $\mathbf{B}_i$ ($\overrightarrow{PB_i}$) expressed in the moving frame, $\mathbf{b}_i$ represents the vector ${}^B\mathbf{b}_i$ expressed in the fixed frame (i.e., $\mathbf{b}_i = {}^AR_B\,{}^B\mathbf{b}_i$), $\mathbf{s}_i$ is a unit vector pointing from $\mathbf{A}_i$ to $\mathbf{B}_i$, and d_i is the length of cable i. Solving Eq. (2.6) for $\mathbf{s}_i$, we obtain

$$\mathbf{s}_i = \frac{\mathbf{p} + \mathbf{b}_i - \mathbf{a}_i}{d_i} \tag{2.7}$$

where

$$d_i = |\mathbf{p} + \mathbf{b}_i - \mathbf{a}_i| \tag{2.8}$$

For the purpose of analysis of the position of the cable, we assume that each cable is connected to the fixed base by a universal joint such that it cannot rotate about the longitudinal axis. The orientation of each cable with respect to the fixed base can be described by two Euler angles, namely a rotation of ϕ_i about z_i-axis resulting in a (x_i', y_i', z_i') frame, followed by another rotation of θ_i about the rotated y_i'-axis as shown in Figure 2.10. Hence the rotation matrix of the ith cable can be written as:

$${}^AR_i = \begin{bmatrix} c\phi_i c\theta_i & -s\phi_i & c\phi_i s\theta_i \\ s\phi_i c\theta_i & c\phi_i & s\phi_i s\theta_i \\ -s\theta_i & 0 & c\theta_i \end{bmatrix} \tag{2.9}$$

where $s\phi$ denotes sine of angle ϕ while $c\phi$ denotes cosine of angle ϕ. The unit vector

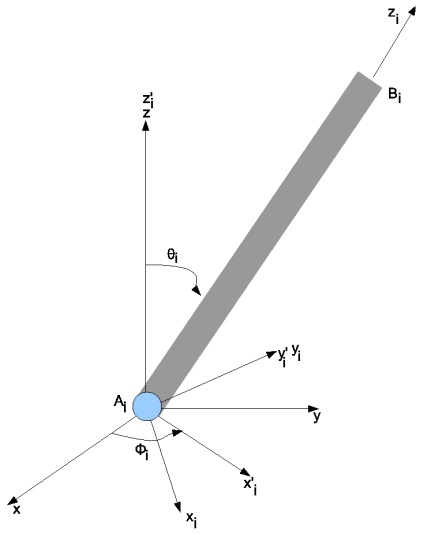

Figure 2.10: *Euler angles of the cable*

along the cable in the coordinate frame (O, x, y, z) is obtained by:

$$\mathbf{s}_i = {}^{A}R_i \, {}^{i}\mathbf{s}_i = {}^{A}R_i \begin{bmatrix} 0 \\ 0 \\ 1 \end{bmatrix} = \begin{bmatrix} c\phi_i s\theta_i \\ s\phi_i s\theta_i \\ c\theta_i \end{bmatrix} \tag{2.10}$$

So the Euler angles ϕ_i and θ_i can be computed as the following:

$$\begin{aligned} c\theta_i &= s_{iz} \\ s\theta_i &= \sqrt{s_{ix}^2 + s_{iy}^2} \qquad (0 \le \theta_i \le \pi) \\ s\phi_i &= s_{iy}/s\theta_i \\ c\phi_i &= s_{ix}/s\theta_i \end{aligned}$$

where s_{ix}, s_{iy} and s_{iz} are the x, y and z components of $\mathbf{s}_i$. Eq. (2.10) in addition with the 4 equations below determine the direction and Euler angles of the ith cable depending on the moving platform location. In this subsection, the geometric analysis of INCA robot was investigated, the length of cables, which is used in dynamics analysis of cable, is computed from the position of the moving platform.

2.2.2 Velocity Analysis

Next, we compute the linear and angular velocities of each cable in term of the velocity and angular velocity of the moving platform. The velocity of the ball point B_i, denoted as $\mathbf{v}_{bi}$, is found by taking the time derivative of the right-hand side of Eq. (2.6):

$$\mathbf{v}_{bi} = \mathbf{v}_p + \omega_p \times \mathbf{b}_i \tag{2.11}$$

Transforming $\mathbf{v}_{bi}$ to the ith cable frame yields:

$${}^{i}\mathbf{v}_{bi} = {}^{i}R_A \, \mathbf{v}_{bi} \tag{2.12}$$

where ${}^{i}\mathbf{v}_{bi} = [{}^{i}v_{bix}, {}^{i}v_{biy}, {}^{i}v_{biz}]^T$ denotes the velocity of B_i expressed in the ith cable frame, and ${}^{i}R_A = {}^{A}R_i^T$. The velocity of B_i can also be written in terms of the angular velocity of the ith cable by taking the derivative of the left-hand side of Eq. (2.6) with respect to time:

$${}^{i}\mathbf{v}_{bi} = d_i \, {}^{i}\omega_i \times {}^{i}\mathbf{s}_i + \dot{d}_i \, {}^{i}\mathbf{s}_i \tag{2.13}$$

Making scalar product both sides of Eq. (2.13) with ${}^{i}\mathbf{s}_i$ yields

$$\dot{d}_i = {}^{i}v_{biz} \tag{2.14}$$

Derivation with respect to time of d_i ($\dot{d}_i$) also can be computed in term of projection of velocity of point B_i on unit vector $\mathbf{s}_i$:

$$\dot{d}_i = \mathbf{s}_i^T (\mathbf{v}_p + \omega_p \times \mathbf{b}_i) \tag{2.15}$$

Since each cable does not spin about its longitudinal axis, $\omega_i^T \mathbf{s}_i = 0$. Left cross-multiplying both sides of Eq. (2.13) by $\mathbf{s}_i$, we obtain the angular velocity vector of the cable i:

$$ {}^i\omega_i = \frac{1}{d_i}({}^i\mathbf{s}_i \times {}^i\mathbf{v}_{bi}) = \frac{1}{d_i}\begin{bmatrix} {}^iv_{biy} \\ {}^iv_{bix} \\ 0 \end{bmatrix} \tag{2.16} $$

The purpose of the velocity analysis of the INCA robot is represent the time derivative of cable's length $\dot{d}_i$ from the position of the moving platform, this value $\dot{d}_i$ is used in analysing cable dynamics.

2.2.3 Acceleration Analysis

The acceleration of point B_i, expressed in the fixed frame i.e., the time derivative of v_{bi} is given in Eq. (2.11):

$$ \dot{\mathbf{v}}_{bi} = \dot{\mathbf{v}}_p + \dot{\omega}_p \times \mathbf{b}_i + \omega_p \times (\omega \times \mathbf{b}_i) \tag{2.17} $$

Expressing $\dot{\mathbf{v}}_{bi}$ in the ith cable frame gives

$$ {}^i\dot{\mathbf{v}}_{bi} = {}^iR_A\, \dot{\mathbf{v}}_{bi} \tag{2.18} $$

The acceleration of B_i can also be expressed in terms of the angular acceleration vector of the ith cable by taking the derivative of Eq. (2.13) with respect to time:

$$ {}^i\dot{\mathbf{v}}_{bi} = \ddot{d}_i\, {}^i\mathbf{s}_i + d_i\, {}^i\dot{\omega}_i \times {}^i\mathbf{s}_i + d_i\, {}^i\omega_i \times ({}^i\omega_i \times {}^i\mathbf{s}_i) + 2\dot{d}_i\, {}^i\omega_i \times {}^i\mathbf{s}_i \tag{2.19} $$

Since the cables do not spin about their own axis, ${}^i\dot{\omega}_{iz} = 0$. Scalar product both sides of Eq. (2.19) by ${}^i\mathbf{s}_i$, we obtain:

$$ \ddot{d}_i = {}^i\dot{v}_{biz} + d_i\, {}^i\omega_i^2 \tag{2.20} $$

Furthermore, the angular velocity vector of cable ith is given in Eq. (2.16), the acceleration $\ddot{d}$ od the cable can be written as:

$$ \ddot{d}_i = {}^i\dot{v}_{biz} + \frac{{}^iv_{bix}^2 + {}^iv_{biy}^2}{d_i} \tag{2.21} $$

Cross-multiplying both sides of Eq. (2.19) by ${}^i\mathbf{s}_i$, we obtain the angular acceleration vector of the cable i:

$$ {}^i\dot{\omega}_i = \frac{1}{d_i}\, {}^i\mathbf{s}_i \times {}^i\dot{\mathbf{v}}_{bi} - \frac{2\dot{d}_i}{d_i}\, {}^i\omega_i = \frac{1}{d_i}\begin{bmatrix} -{}^i\dot{v}_{biy} + \frac{2\,{}^iv_{biz}\,{}^iv_{biy}}{d_i} \\ {}^i\dot{v}_{bix} - \frac{2\,{}^iv_{biz}\,{}^iv_{bix}}{d_i} \\ 0 \end{bmatrix} \tag{2.22} $$

In this thesis, we assume that the cable's mass is negligible and we only account it for the moment of inertia of the motor. Thus, the acceleration of the cable does not effects on our dynamics of the INCA robot, but the computation of acceleration of the cable can be used in the future investigation.

2.3 Dynamics of the INCA robot

2.3.1 Modelling of elastic cables

In this subsection, we investigate the dynamics of the cable. According to the Figure (2.11) the cable model should receive the motor angles, the cable length as the inputs. The outputs are the tensions of the cables, which drive the moving platform. For this

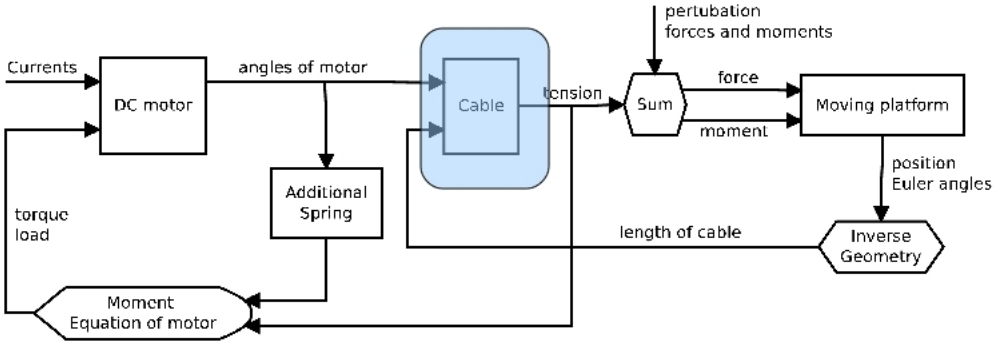

Figure 2.11: *Block diagram of INCA robot dynamics: Dynamics of cable*

purpose, a simplified elastic model of cable is proposed to determine cable behaviour. In this model, we account for the elasticity and the damping effect of the cable. However, the dynamic effects of cable mass are neglected, but the cable mass itself is accounted in the moment of inertia of motor, which will be dealt with in next section. With this assumption, the model that contains the cable elastic and damping behaviour is generated and the method to determine the internal forces in cable direction is presented in this section.
Hooke's law provides the relationship between the tensile stress σ and the strain (or relative elongation) ε:

$$\sigma = E\,\varepsilon \tag{2.23}$$

where E is the Young modulus of the material. Thus, the tension T_e within the cable elastic behaviour acting in the cable direction, is modelled by a linear function of the strain within and the axial stiffness of the cable:

$$T_e = ES\varepsilon \tag{2.24}$$

$$\varepsilon = \frac{d - d_0}{d_0} \tag{2.25}$$

where d is the length of the cable which is computed in previous section, $d_0(t)$ is the no-load length of the active part of the cable, varying due to the rotation of the roller, S is the cross section area of the cable element. For explanation of the difference between

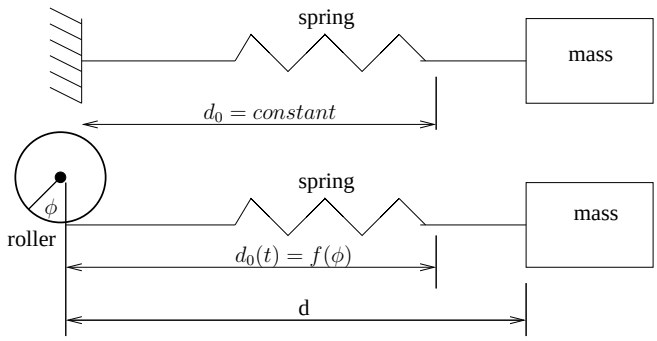

Figure 2.12: *No-load length of fixed cable and of the cable attracted to active roller*

the no-load length and no-load length of the active part of the cable, in Figure 2.12, we represent 2 cases of no-load length of cable. In the first case, a cable is fixed in one side and connected to moving platform in the other side, the its elasticity is considered as a spring with constant no-load length (or whole the no-load length is active). However in second case, the cable is attracted with the active roller, its elasticity is considered as a spring with varying no-load length (or only the part outside the roller of cable is active).
The variation of $d_0(t)$ only depends on the action of roller. During a small winding process of time length δt, the length of cable δd is stored, with:

$$\delta d = \delta d_0(1 + \varepsilon) \tag{2.26}$$

This corresponds to a rotation of the winder of $\delta\varphi$, which can be written as:

$$\delta\varphi = \frac{\delta d}{R} \tag{2.27}$$

where R is the radius of the motor's drum, yielding:

$$\frac{\delta d_0}{\delta t} = -\frac{R\dot{\varphi}}{1 + \varepsilon} \tag{2.28}$$

Under the assumption that the cable is stored with its original strain, let's introduce $\varepsilon_s(\alpha, t)$, where α is the position along the roll. During a rolling phase, denoting $\alpha = 0$ the position where the cable leaves the roll, we have $\varepsilon_s(\alpha, t) = \varepsilon(t)$. During an unrolling phase ($\dot{\varphi} < 0$), the cable that was previously stored is restored, yielding :

$$\frac{\delta d_0}{\delta t} = -\frac{R\dot{\varphi}}{1 + \varepsilon(0, t)} \tag{2.29}$$

From Eq. (2.25) and under the assumption that the unrolling and rolling process have no difference, we can write two equations (2.28) and (2.29) as state equation for d_0:

$$\dot{d_0} = -\frac{R\, w\, d_0}{d} \tag{2.30}$$

where w is the angular velocity of motor, $w = \dot{\varphi}$ is also the state equation for φ.
The friction between the braids of the cable, along with the polymer coatings creates

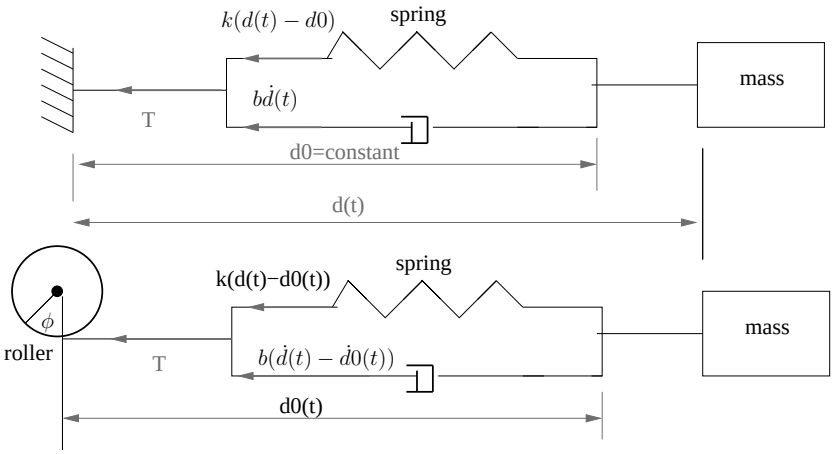

Figure 2.13: *Tension of fixed cable and of the cable attracted to active roller*

damping effect. This effect is assumed to be linear with the following relationship between strain rate and damping force. The forces in the cable generated by damping are:

$$T_d = b.\Delta\dot{d} = b(\dot{d} - \dot{d}_0) \tag{2.31}$$

where $\Delta\dot{d}$ is the rate of the cable length stretching, $\dot{d}$ is rate of real length of cable, computed in Eq. (2.14), $\dot{d}_0$ is rate of unload length of the cable, introduced in Eq. (2.30) and b is the damping coefficient of the cable. The tension of cable, T, within the elastic damping behaviour can be obtained:

$$T = T_e + T_d \tag{2.32}$$

The cable should be under tension, thus internal force in cable should be greater than 0. In this section, a dynamic model of cable is introduced where the tension of cable is obtained from the winding or unwinding angle of motor, length of cable and its derivative. These tensions are considered as forces applied on the moving platform.

2.3.2 Dynamics of the moving platform

The moving platform of INCA robot is considered as a 6 degrees of freedom rigid body with a fixed mass and inertia. The translational motion of the moving platform coordinate frame is given below, where the applied forces $F_p = [F_{px}, F_{py}, F_{pz}]^T$ are in the moving platform frame, and the mass m of the body is constant.

$$\dot{\mathbf{v}}_p = \frac{F_p}{m} - \omega_p \times \mathbf{v}_p \tag{2.33}$$

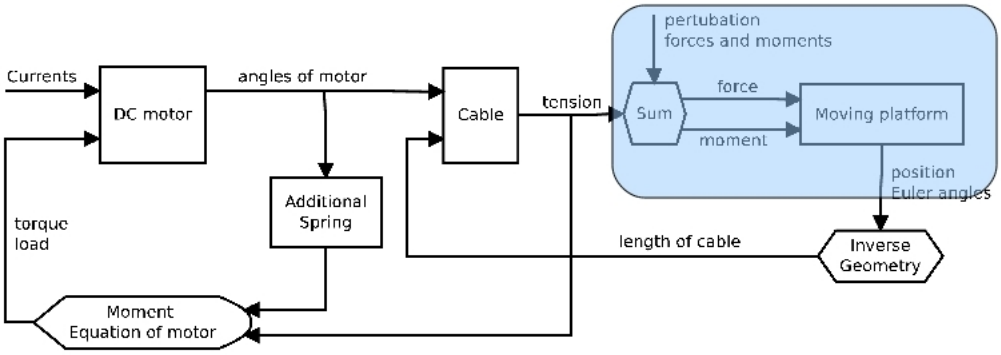

Figure 2.14: *Block diagram of INCA robot dynamics: Dynamics of moving platform*

The rotational dynamics of the moving platform frame are given below, where the applied moments are M_p, and the inertia tensor I is with respect to the origin P.

$$\dot{\omega}_p = I^{-1}(M_p - \omega_p \times (I\omega_p)) \tag{2.34}$$

where M_p and F_p are respectively the applied forces and the moments in the moving platform frame, due to the tensions of the 8 cables, the gravity force on the moving platform, the external disturbance forces and moments caused by these forces. M_p and F_p can be written as:

$$F_p = -\sum_{i=0}^{8}(T_i\,{}^B\mathbf{s}_i) + \begin{bmatrix} 0 \\ 0 \\ -g.m \end{bmatrix} + G_p \tag{2.35}$$

$$M_p = \sum_{i=0}^{8}({}^B\mathbf{b}_i \times (T_i\,{}^B\mathbf{s}_i - G_p)) \tag{2.36}$$

where T_i is the tension of cable ith, ${}^B\mathbf{s}_i = {}^AR_B^T\,\mathbf{s}_i$ is the unit vector of cable in moving platform frame, G_p is the external disturbance forces, ${}^B\mathbf{b}_i$ is the vector from the centre of mass P to the connector B_i, expressed in moving platform frame.

2.3.3 Modelling of the actuator

In INCA robot, the moving platform is driven through 8 cables by 8 actuator systems, each actuator system includes one DC motor and additional spring system. The DC motor is coupled with 2 drums (rollers) that provide translational motion to cable and additional spring system in two different directions. Additional spring systems keep initial tensions in cable and help reducing load for motors. The mechanic equation of DC motor can be written from Newton's law:

$$J_m\dot{w} + \tau_f = \Gamma \tag{2.37}$$

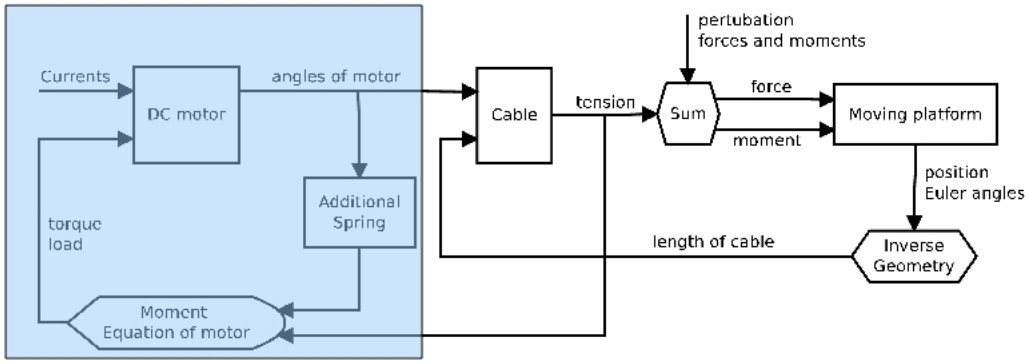

Figure 2.15: *Block diagram of INCA robot dynamics: Dynamics of actuator*

where J_m is moment of inertia of the motor and the other elements connected to it, τ_f is friction torque the mechanical system of the motor, K_t is electromotive force constant of motor, Γ is torque applied in motor and w is angular velocity of motor. The friction torque, $\tau_f(t)$, is modelled to include many of the friction phenomena encountered in practice, among other things so-called Coulomb friction and viscous friction.

$$\tau_f = b_v w + b_c sign(w) \tag{2.38}$$

where b_v and b_c are the viscous and the Coulomb friction coefficients, sign(w) is signed function of w. Coulomb friction torque can also be written in term of friction smoothness coefficient β, Eq. (2.38) becomes:

$$\tau_f = b_v w + b_c \tanh(\beta w) \tag{2.39}$$

Γ includes the motor torque Γ_m and the torque load Γ_l from tension of cable and additional spring:

$$\Gamma = \Gamma_m + \Gamma_l \qquad \text{where} \qquad \Gamma_l = T.R - F_s.R_s \tag{2.40}$$

Motor torque Γ_m is related to the armature current, i, by a constant factor K_t: $\Gamma_m = K_t\, i$. R and R_s respectively are the radius of the rollers attached to the cable and the additional spring. T is the tension of the cable, F_s is the elastic force of the additional spring which can be computed by the following equation:

$$F_s = -k_s R_s \varphi + \frac{R_s}{R} T_{t=0} \tag{2.41}$$

where k_s is spring constant of additional spring, $T_{t=0}$ is the initial tension of cable.

2.4 Simulation of system

In this section, the dynamic model of INCA robot, introduced in the previous section, was implemented in a S-function in Matlab. The inputs are the currents applied to each motor. The parameters some are obtained by measurement or from the data-sheet of the INCA robot and others are given arbitrarily. The output of simulation model can be decided in S-function file. Moreover, to make the simulation visible and to use in visual control of INCA robot, a program which animates INCA robot in simulation was developed. The animated data can be saved and replayed.

List of parameters used in simulation

The parameters used in simulation are obtained different means, are given in Table (2.1). The parameters given by measurement of Prof. Jacques Gangloff, are noted as 'Measurement' in the Source column. The geometric parameters, the moving platform and the motor's parameters, obtained from the data-sheets provided by Haption and Maxon, are noted as 'Datasheet' in the Source column. The rest of parameters, given arbitrarily, is announced as 'Arbitrary'. The positions of point A_i are compound to the positions of the centre of the free rotational pulley, expressed in fixed base coordinate, which is introduced in the previous section. The position of joint ${}^bB_i$ is defined similarly, from the structure datasheet of the moving platform, expressed in the moving platform frame. The initial position and Euler angles of moving platform in fixed base frame are chosen respectively $(0, 0, 1.43)$ and $(0, 0, 0)$. The Table (2.1) on page 24 presents a list of the parameters used in the simulation and their source.

The initial states such as velocities and angular velocities of the moving platform and motor are equal 0, the initial states of the no-load length of the cables is computed from the initial tensions of the cables $T_c(t = 0)$, the length and the elastic modulus of the cable. We consider that the tension of the cable $T_c(t = 0)$ is equal the elastic tension of the additional spring $T_s(t = 0)$ in the static state.

[1]The moment of inertia attached to the DC motor is computed from moment of inertia of its rotor and the cables attached it. The value of moment of inertia J should include other rotating objects, such as pulleys, rollers, conveyors of potentiometer, etc. In this simulation the value of J only accounts for the inertia of the rotor and the masses of the cables and the spring

Parameter	Symbol	Value	Source
Radius of the roller 1 (mm)	R	17.5	Datasheet
Radius of the roller 2 (mm)	R_s	6	Datasheet
Stiffness of additional spring (N/m)	k_s	16	Measurement
Elastic modulus of cable (N.m/m)	λ	32224	Measurement
Damping coefficient of cable (N/m/s)	b	10	Arbitrary
Moment of inertia (kgm^2)	J	$3.0563.10^{-5}$	Computed [1]
Viscous friction coefficient	b_v	$0.3.10^{-3}$	Arbitrary
Coulomb friction coefficient	b_c	0.005	Arbitrary
Smooth coefficient of friction	β	0.8	Arbitrary
Motor torque constant (Nm/A)	K_t	0.0603	Datasheet
Mass of moving platform (kg)	m	0.1725	Datasheet
Moment of inertia of MP (kgm^2)	I	$\begin{bmatrix} 0.8 & 0 & 0 \\ 0 & 1.5 & 0 \\ 0 & 0 & 1.8 \end{bmatrix} 10^{-4}$	Datasheet

Table 2.1: *List of the parameters used in simulation*

Simulation results

In the following simulation, we apply a current 2A in motor number 1, the seven other motors having no current. The position of the moving platform, the angles of the 8 motors and the tensions in 8 cables are represented in Figure (2.16).[2] To illustrate the dynamics of the moving platform, the actuators and the cables, the outputs of the simulation include: 3 element vector of the moving platform's position in 3 axes, 3 roll pitch yaw rotation angles of the moving platform, 8 angles of the DC motors, 8 tensions of the cables. All of result outputs is shown in the following figures:

[2]We define the positive value of the current makes the roller wind the cable, the positive value of the angle of motor winds the cable.

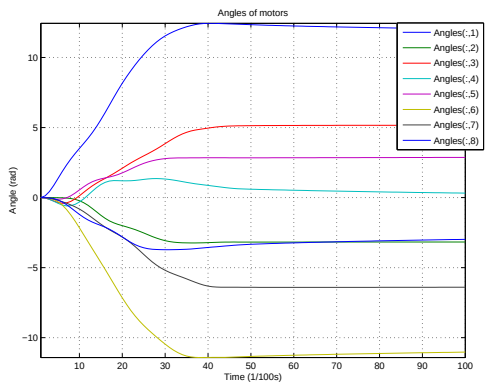

(a) *Angles of the motors*

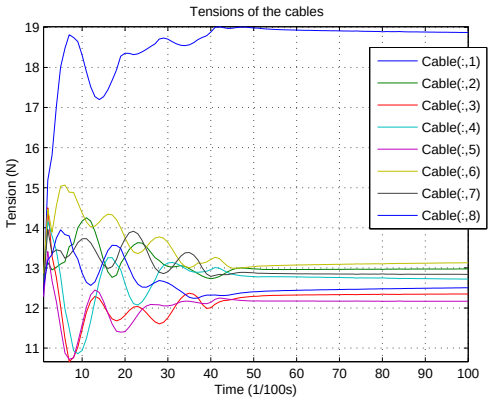

(b) *Tensions of the cables*

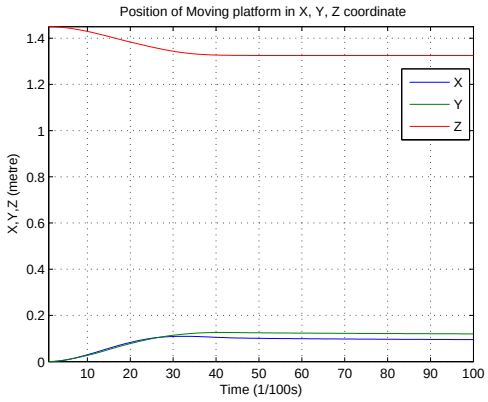

(c) *Position of moving platform*

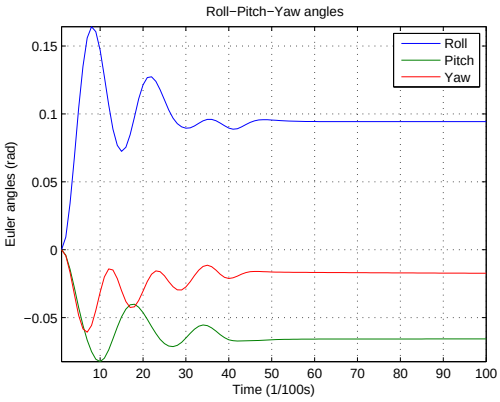

(d) *Angles of the motors*

Figure 2.16: *Outputs of simulation*

Chapter 3

Identification of the parameters of the INCA robot

Contents

Figure 3.1 shows an algorithm for modelling and system identification. The process of identification for INCA robot follows this algorithm. System identification is an iterative process and it is often necessary to go back and repeat earlier steps. This is illustrated with arrows in the figure. Notice that the order of the blocks in the algorithm does not only describe the chronological order the tasks are performed, but also how they influence each other. For example, a certain model structure can be proposed by the physical model, the amount of data limits the model complexity, etc.

3.1 Non-linear Grey-box identification

In this section, non-linear grey-box identification problem is briefly described, and we also want to discuss about some problems in identification INCA robot.

3.1.1 Introduction to grey box identification

Generally, the user has two sources of information on which to base the model making: prior knowledge and experiment data. The idea of "grey-box" identification is to use both sources in order to estimate parameters for a class of models which follows prior knowledge. In other words, the goal is to find a parametric model which fits given experiment data with the minimum loss according to a given criterion. The starting point for the nonlinear grey-box identification is the continuous-time state-space model structure that was introduced in chapter 2.

$$\begin{aligned} \dot{x}(t) &= f(t, x(t), \wp, u(t)) \\ y(t) &= h(t, x(t), \wp, u(t)) + e(t) \end{aligned} \tag{3.1}$$

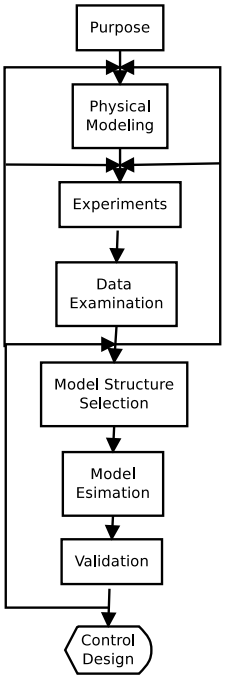

Figure 3.1: *Algorithm for modelling and system identification*

where f and h are nonlinear functions. $x(t)$ is the state vector, $u(t)$ and $y(t)$ are input and output signals, $e(t)$ is disturbance signal, and t denotes time. Finally $\wp$ is the vector of unknown parameters. Given a set of input/output-data the aim is to determine the parameter vector that minimizes a criterion such as

$$\Lambda_N(\wp) = \frac{1}{N} \sum_{t=1}^{N} |\varepsilon(t, \wp)|^2 \tag{3.2}$$

where $\varepsilon(t)$ denotes the prediction error

$$\varepsilon(t, \wp) = y(t) - \hat{y}(t, \wp) \tag{3.3}$$

The experiments in this thesis utilized the non-linear grey-box model structure IDNLGREY, available in the System Identification Toolbox of MATLAB. The model can be either a discrete or continuous-time state-space model, and it is defined in a Matlab m-file or mex-file. The purpose of the model file is to return the state derivatives and model outputs as a function of time, states, inputs, and model parameters. The prediction $\hat{y}(t, \wp)$ then becomes the simulated output of the model described in Eq.(3.1) with the input $u(t)$ (without $e(t)$) for the current parameter vector $\wp$. The data set, (y, u), is put into an IDDATA object and $\wp$ is estimated by applying

a prediction error method, which performs a numerical optimization of the criterion shown in Eq.(3.2) by an iterative numerical search algorithm. This search algorithm involves simulation of the system for different values of $\wp$. The user specifies an initial parameter vector and it is also possible to fix some components in $\wp$. To speed up the numerical optimization, the simulation model is implemented in a mex-file (C-code).

3.1.2 Problems in identification for the INCA robot

In this project, the nonlinear grey-box model of the INCA robot given in previous section will be defined by a Matlab m-file: "*INCA6D_ m.m*". Unknown IDNLGREY model parameters and initial states will be estimated using measured or simulated data with command "**pem**". Algorithm and additional properties for estimation can be chosen. Table 3.1 describes the nonlinear grey-box model of the INCA robot, used in estimation where the 8 inputs are the 8 currents applied to 8 motors, The 8 outputs

Table 3.1: *Description of nonlinear grey-box model of the INCA robot in Matlab*

```
Time-continuous nonlinear state-space model defined by 'INCA6D' (m-file):
               dx/dt = F(t, u(t), x(t), p1, ..., p9)
               y(t) = H(t, u(t), x(t), p1, ..., p9) + e(t)
 with 8 inputs, 36 states, 8 outputs, and 5 free parameters (out of 11).
```

are the 8 angles of the 8 motors measured by encoders, The 36 states are

- 3 entries for the position of centroid of moving platform in fixed base frame
- 3 entries for the translational velocity of moving platform in body-fixed frame
- 3 rotation Euler angles of moving platform in fixed base frame
- 3 the angular rates of moving platform in body-fixed axes
- 8 angles of 8 motors
- 8 angular velocities of 8 motors
- 8 no-load length of cables

Nonlinear grey-box model of INCA robot includes 11 parameters:

- R - Radius of roller in cable side
- R_s - Radius of roller in additional spring side
- k_s - spring constant of additional spring

- m - mass of moving platform
- J_m - moment of inertia to motor
- K_t - torque constant of motor
- b_v - viscous friction coefficient of motor
- b_c - Coulomb friction coefficient of motor
- β - Friction smoothness coefficient
- b - damping coefficient of cable
- λ - elastic modulus of cable

In order to reduce the computation of the estimation, we assume that the parameters of all the cables (and motors) are equal, moreover we do not include 3×3 inertia matrix. However, there are some problems in the model that make difficult to obtain high accuracy in the identification.

- Firstly, INCA model includes flexibilities, damping and friction parameters which are difficult to determine, because of their lack of effect on the output, especially damping coefficient of cable.
- Secondly, 8 initial states of no-load length of cables can not be measured and have physical dependences from the initial position of the platform and several parameters such as λ, k_s. This closed loop connection of initial states and parameters is a sensitive condition to validate the estimated model and also makes a constrain for the user in choosing initial value of initial states and parameters for identification.
- Finally, cables have one unique property - they can pull but not push, so the tension in cable must greater than 0. This constrain requires special care when choosing input signals and initial values for estimation, and sometimes causes troubles in estimation and validation when the result model does not satisfies this constrain.

Therefore in the following work, an identification method is proposed, in which the procedure is divided into 2 steps:

- First, the estimation is performed using simulated data with modified initial values for initial states for parameter. The results are analysed to decide identifiability of each parameter.
- Second, the most efficient procedure, included the input signal, the criterion is chosen to apply in the estimation using the experiment data

3.2 Identification with simulated data

In this section, the estimation procedure is applied for the simulated data, in order to investigate the sensitivity of each parameters. The model used to give the simulated data is the grey-box model used for estimation, therefore the identification for the simulated data is white-box identification. However, to investigate the effects of noise in the estimation process, we also apply noise in the "sensors" of simulation.

3.2.1 Input - Output

The input chosen for the identification of the INCA robot must satisfy following conditions:

- Proper excitation: The identification gives an accurate model at the frequencies where the input signal contains much energy. We say that the input signal has good excitation at these frequencies. Thus, the good input signal used in identification must have a large energy content in a large frequency range. In this project, the pseudo-random binary sequence (PRBS) is the choice of input signal.
- Maintain positive tension on the cables: To prevent the negative tension of cable, applying a reasonable input could avoid the negative tension in the cable. The currents should be lifted up so that the minimum value of the current is greater than 0.
- Satisfy the safety condition for motors and cables: The current applied to motor must be smaller than the value of the maximum continuous current of motor, and the tension in cable must be under safe allowable tensions of the cable.

According to these conditions, Figure 3.2 on page 32 represents the input signals using in simulation. Actually, these input signals are acquired directly from DC motors of the INCA robot when we apply the PRBS signals as the reference for currents. The current reference is a 4 bit PRBS, with the period is 0.25s, the minimum value of the current reference is 0.5A and the maximum is 1A. Table 3.2 on page 33 represents list of parameters used in the simulation. The output using in identification (acquired from simulation, in this case) must allow to identify the dynamics of the system, and must measurable from the 'real' INCA robot. In this project, the angles of the DC motors driving cables are chosen to be the output. The simulated output data is shown in the Figure 3.3 on on page 34.

3.2.2 Method and Criterion

The estimation method used for identification of the INCA robot is an iterative prediction-error minimization method (it uses an iterative algorithm to minimize a

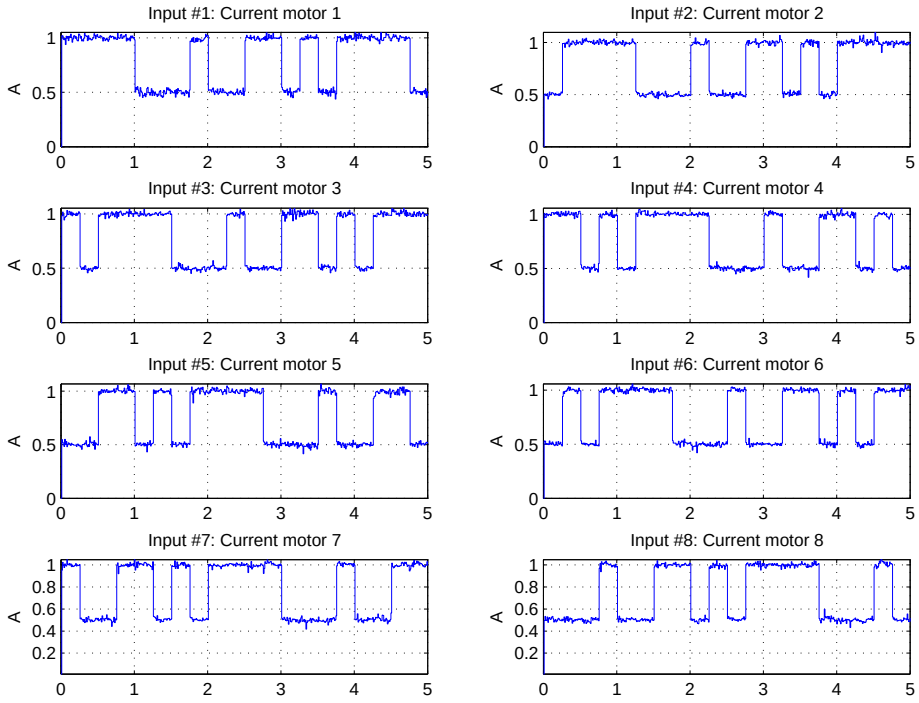

Figure 3.2: *Simulated input signals: Currents of motors*

cost function). In Matlab, the iterative estimation command is `pem`. Following the Matlab reference, there are two categories of methods available for nonlinear grey-box modelling.

- One category of methods consists of the minimization schemes that are based on line-search methods, including Gauss-Newton type methods, steepest-descent methods, and Levenberg-Marquardt methods.
- The Trust-Region Reflective Newton method of nonlinear least-squares (`lsqnonlin`), where the cost is the sum of squares of errors between the measured and simulated outputs, which is defined in the Eq. (3.2). This method requires Optimization Toolbox software.

According to these methods, in Matlab, there are 2 specifies criterion used during minimization of the cost function:

- 'Det': Minimize $|\varepsilon^T \varepsilon|$ where ε represents the prediction error. This is the optimal choice in some statistical senses and leads to the maximum likelihood estimates

Parameter	Symbol	Value
Radius of the roller 1 (mm)	R	17.5
Radius of the roller 2 (mm)	R_s	6
Stiffness of the additional spring (N/m)	k_s	16
Elastic modulus of cable (N.m/m)	λ	25000
Damping coefficient of cable (N/m/s)	b	8
Moment of inertia (kgm^2)	J	8.10^{-5}
Viscous friction coefficient	b_v	0.0002
Coulomb friction coefficient	b_c	0.005
Smooth coefficient of friction	β	0.8
Motor torque constant (Nm/A)	K_t	0.08
Mass of moving platform (kg)	m	0.1725
Moment of inertia of MP (kgm^2)	I	$\begin{bmatrix} 0.8 & 0 & 0 \\ 0 & 1.5 & 0 \\ 0 & 0 & 1.8 \end{bmatrix} 10^{-4}$
Initial position of moving platform (m)	$[x, y, z]_{t=0}$	$[0, 0, 1.43]$
Initial Euler angles of moving platform (rad)	$[\phi, \theta, \psi]_{t=0}$	$[0, 0, 0]$

Table 3.2: *List of parameters used to obtain simulated data*

in case nothing is known about the variance of the noise. It uses the inverse of the estimated noise variance as the weighting function.

- 'Trace': Minimize the trace of the weighted prediction error matrix trace($\varepsilon^T \varepsilon W$), where ε is the matrix of prediction errors, with one column for each output, and W is a positive semi-definite symmetric matrix of size equal to the number of outputs. By default, W is an identity matrix of size equal to the number of model outputs, so the minimization criterion becomes trace($\varepsilon^T \varepsilon$), or the traditional least-sum-of-squared-errors criterion.

There are 2 quantitative criteria used to evaluate the quality of the estimated model:

- fit: percentage of fitting between output data, and output of estimated model with the same input

$$\text{fit} = 100 \frac{1 - \text{norm}(y_h - y)}{\text{norm}(y - \text{mean}(y)))} \tag{3.4}$$

- Value of the loss function, equal to $|\varepsilon^T \varepsilon / N|$, where ε is the residual error matrix (one column for each output) and N is the total number of samples.

$$\text{LossFcn} = \frac{1}{N} \sum_{1}^{N} \varepsilon(t, \wp_N)^T \varepsilon(t, \wp_N) \tag{3.5}$$

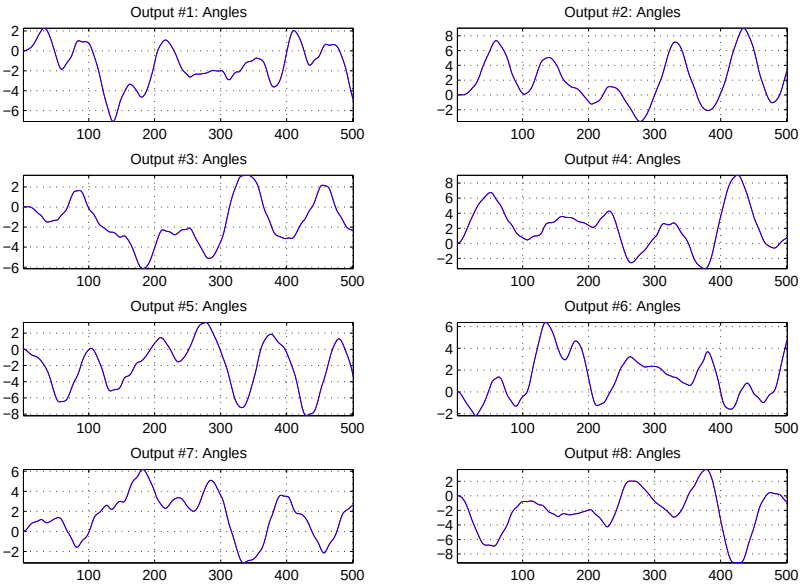

Figure 3.3: *Simulated output signals: Angles of motors*

In this section, the methods and the algorithms used for estimation parameters and the quantitative descriptions of the model quality are introduced. The result of the estimation from the simulated data is analysed based on these criteria.

3.2.3 Results and Conclusion

In order to analyse the effect of noise to the identification, the trial data is divided into 2 groups: without noise and with noise. Furthermore, we have observed that not all the values of parameters can be measured or included in data-sheet. Thus, to investigate the sensitivity of each parameter and the influence of number of estimated parameters on the identification result, the identification trial must be processed 2 times: the first time, all the parameters is estimated, and the second time, we only estimate the unknown parameters, which are noted as 'Arbitrary' in the Table (2.1) on page 24. Moreover, before each identification process, the initial values for the parameters and initial states are provided. The influence of these initial value on the identification also need to be analysed. Therefore, in order to investigate all the possible factors which have effect on the identification result, we propose the following set of trials:

1. Trial.1: Estimation of all the parameters, data without noise, large error in initial value

2. Trial.2: Estimation of the unknown parameter, data without noise, large error in initial value

3. Trial.3: Estimation of the unknown parameter, data without noise, small error in initial value

4. Trial.4: Estimation of the unknown parameter, data with noise [1], small error in initial value

	Estimated parameters	**Initial value**	**Noise**
Trial.1	All	Large error	Without noise
Trial.2	Unknown	Large error	Without noise
Trial.3	Unknown	Small error	Without noise
Trial.4	Unknown	Small error	With noise

The identification result of each trial is presented in the next subsections.

[1] The noise is supplied by adding to each sample of the outputs a random value ranging between ±5% of the sample of the outputs itself

Trial.1: Estimation of all the parameters, data without noise, large error in initial value

Parameter	Value	Initial	Estimated	Fitting
R	0.0175	0.0175	0.0199	86.3%
R_s	0.006	0.006	0.0070	83.3%
k_s	16	16	17.189	93.1%
λ	25000	31250	36171.1	55.3%
b	8	16	2.2650	28.7%
J	0.00008	0.0001	0.00011	62.5%
b_v	0.0002	0.00017	0.00027	65.0%
b_c	0.005	0.004	0.00697	62.0%
β	0.8	1	0.8075	99.1%
K_t	0.08	0.08	0.1099	62.5%
m	0.1725	0.1725	0.1725	100%
$[x, y, z]_{t=0}$	$[0, 0, 1.43]$	$[0.025, 0.025, 1.5]$	$[0.003, 0.0, 1.421]$	99.3%

Table 3.3: *Trial.1: List of estimated parameters*

Output	Fitting (%)
Angle of motor 1	97.75
Angle of motor 2	97.16
Angle of motor 3	98.33
Angle of motor 4	97.67
Angle of motor 5	97.08
Angle of motor 6	97.78
Angle of motor 7	98.35
Angle of motor 8	97.75
Summary	97.74
Loss function	$7.423.10^{-26}$ [2]
	$2.98.10^{-5}$ [3]

(a) *Fitting result of output*

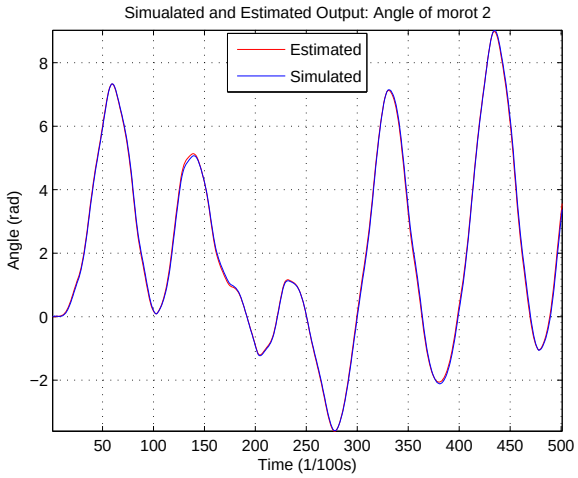

(b) *Simulated - estimated angle of motor 2*

Figure 3.4: *Trial.1: Comparison between simulated data and estimated model output*

[1] Loss function is presented in Matlab
[2] Loss function is computed from the Eq. (3.5)

Trial.2: Estimation of the unknown parameter, data without noise, large error in initial value

Parameter	Value	Initial	Estimated	Fitting
R	0.0175	(fix)	(fix)	(fix)
R_s	0.006	(fix)	(fix)	(fix)
k_s	16	(fix)	(fix)	(fix)
λ	25000	31250	29177.9	83.3%
b	8	16	13.35	not fit
J	0.00008	0.0001	$7.79.10^{-5}$	97.4%
b_v	0.0002	0.00017	0.000197	98.5%
b_c	0.005	0.004	0.00505	99.0%
β	0.8	1	0.7396	92.5%
K_t	0.08	(fix)	(fix)	(fix)
m	0.1725	(fix)	(fix)	(fix)
$[x, y, z]_{t=0}$	$[0, 0, 1.43]$	(fix)	(fix)	(fix)

Table 3.4: *Trial.2: List of estimated parameters*

Output	Fitting (%)
Angle of motor 1	97.77
Angle of motor 2	97.29
Angle of motor 3	98.37
Angle of motor 4	97.94
Angle of motor 5	97.13
Angle of motor 6	97.77
Angle of motor 7	98.42
Angle of motor 8	97.92
Summary	97.82
Loss function	$1.1644.10^{-27}$ [4]
	$3.766.10^{-6}$ [5]

(a) *Fitting result of output*

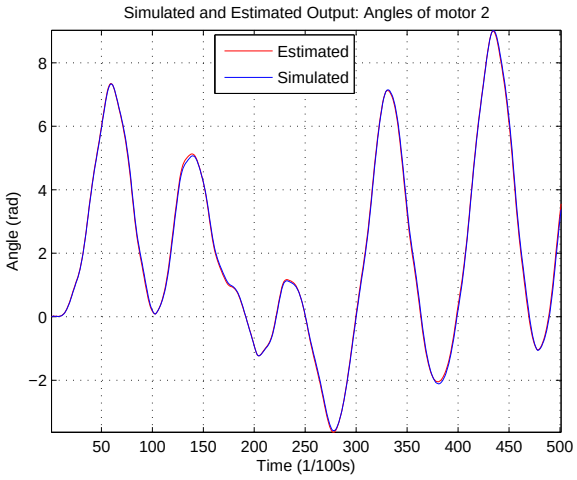

(b) *Simulated - estimated angle of motor 2*

Figure 3.5: *Trial.2: Comparison between simulated data and estimated model output*

[3] Loss function is presented in Matlab
[4] Loss function is computed from the Eq. (3.5)

Trial.3: Estimation of the unknown parameter, data without noise, small error in initial value

Parameter	Value	Initial	Estimated	Fitting
R	0.0175	(fix)	(fix)	(fix)
R_s	0.006	(fix)	(fix)	(fix)
k_s	16	(fix)	(fix)	(fix)
λ	25000	26250	25598.3	97.6%
b	8	7.2	17.036	not fit
J	0.00008	$8.4.10^{-5}$	$7.78.10^{-5}$	97.4%
b_v	0.0002	0.00019	0.000197	98.5%
b_c	0.005	0.00475	0.00506	98.8%
β	0.8	0.84	0.7374	92.1%
K_t	0.08	(fix)	(fix)	(fix)
m	0.1725	(fix)	(fix)	(fix)
$[x, y, z]_{t=0}$	$[0, 0, 1.43]$	(fix)	(fix)	(fix)

Table 3.5: *Trial.3: List of estimated parameters*

Output	Fitting (%)
Angle of motor 1	97.74
Angle of motor 2	97.28
Angle of motor 3	98.39
Angle of motor 4	97.95
Angle of motor 5	97.13
Angle of motor 6	97.75
Angle of motor 7	98.44
Angle of motor 8	97.93
Summary	97.83
Loss function	$1.3263.10^{-27}$ [6]
	$3.744.10^{-6}$ [7]

(a) *Fitting result of output*

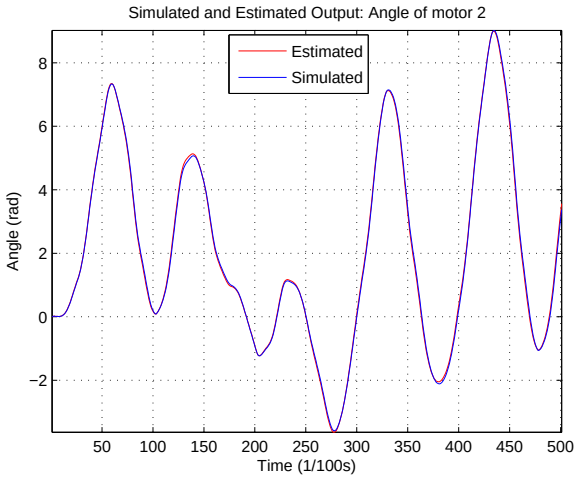

(b) *Simulated - estimated angle of motor 2*

Figure 3.6: *Trial.3: Comparison between simulated data and estimated model output*

[5] Loss function is presented in Matlab
[6] Loss function is computed from the Eq. (3.5)

Trial.4: Estimation of the unknown parameter, data with noise, small error in initial value

Parameter	Value	Initial	Estimated	Fitting
R	0.0175	(fix)	(fix)	(fix)
R_s	0.006	(fix)	(fix)	(fix)
k_s	16	(fix)	(fix)	(fix)
λ	25000	26250	25392.6	98.4%
b	8	7.2	19.0473	not fit
J	0.00008	$8.4.10^{-5}$	$7.78.10^{-5}$	97.4%
b_v	0.0002	0.00019	0.000197	98.5%
b_c	0.005	0.00475	0.00506	98.8%
β	0.8	0.84	0.741	92.1%
K_t	0.08	(fix)	(fix)	(fix)
m	0.1725	(fix)	(fix)	(fix)
$[x, y, z]_{t=0}$	$[0, 0, 1.43]$	(fix)	(fix)	(fix)

Table 3.6: *Trial.4: List of estimated parameters*

Output	Fitting (%)
Angle of motor 1	97.77
Angle of motor 2	97.32
Angle of motor 3	98.42
Angle of motor 4	97.97
Angle of motor 5	97.16
Angle of motor 6	97.78
Angle of motor 7	98.47
Angle of motor 8	97.96
Summary	97.85
Loss function	$1.878.10^{-20}$ [8]
	$5.590.10^{-6}$ [9]

(a) *Fitting result of output*

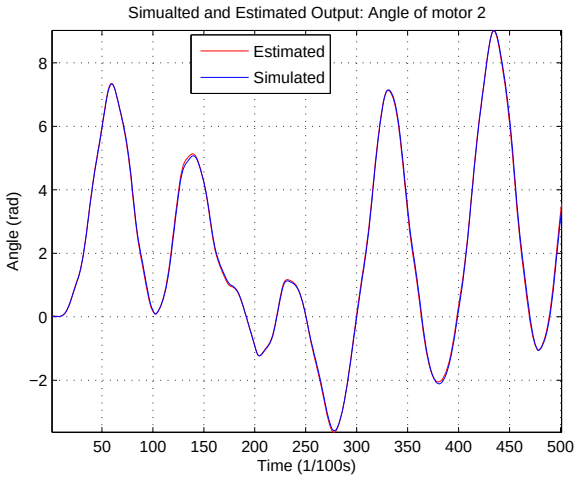

(b) *Simulated - estimated angle of motor 2*

Figure 3.7: *Trial.4: Comparison between simulated data and estimated model output*

[7] Loss function is presented in Matlab
[8] Loss function is computed from the Eq. (3.5)

Conclusions

In the identification trials with the simulated data, we use the same model for simulation and estimation. Thus, in the sequence, the results of the fitting percentage of the outputs will have very small difference, that can be observe on Table (3.3), Table (3.4), Table (3.5) and Table (3.6). However, comparing between the results of each of the estimated parameter of the 4 trials, we can observe significant differences. It reveals the influences of the 3 factors mentioned above on the identification result: the number of estimated parameters, the initial value provided before the identification, and the noise from the simulated data. In this section, the influences of each factor are investigate in order to obtain the most efficient procedure for the identification from the measured data.

The influence of the number of estimated parameters on the identification result: In the trial (1), all the parameters and the initial states are estimated, in others trials, we only estimated the unknown parameters which are not provided from the measurement of Prof. Jacques Gangloff and from datasheet. Comparing the fitting percentages of estimated parameters and parameters used in simulation from Table (3.3) on page 36 and from Table (3.4) on page 37, we can realise that some estimated parameters are not fit the value of simulated parameters in Table (3.3), despite the estimated outputs are fitting with the simulated outputs. That can be explained by 2 reasons:

- the sensitivity of each parameter to the identification process are not similar. The parameters which have significant influences on the dynamic behaviour of the output, will be estimated accurately in the identification. And on the contrary, the parameters which their varying have no effect on the output, will not be estimated accurately. For example, the estimated value of damping coefficient of the cable do not fit with the simulated value in all trials, because of its lack of effect on the dynamics of output.

- some parameters have the same meaning in the dynamic model of the INCA robot. For example, the stiffness of the additional spring, the elastic modulus of cable both represent for the elasticity of the dynamic system. Therefore 4 parameters: R, R_s, k_s and λ can be replaced by one parameter denotes the radius of the roller, and one parameter represents the elasticity of both additional spring and the cable, without changing the dynamics of the system.

The influence of the initial value, provided before the identification: In the trial (2) and trial (3), the numbers of estimated parameters are the same, both input and output data include no noise, only the initial value provided for each parameter before the identification process are different. In the trial (2), the errors between the

initial values of parameters and the simulated parameters are larger than in trial (3) (25% and 5%). Comparing the results of both trials, we can observe the improvement of fitting percentage of estimated parameters in the trial (3): for example, λ from 83% in trial (1) to 98% in trial (2). The reason of the improvement of the result could be the prevention of localized minimal in the optimization of the estimation the model parameters by choosing 'good' initial value for identification.

The influence of the noise on the identification result: In trial (3) and trial (4), all the conditions for the identification process are similar, but we supply a noise on the output signals in the trial (4). The signal-to-noise ratio is 5%. However, the identification results in trial (4) are even better than the results in the trial (3). In a stochastic context, the parameters are random. The sensitivity with respect to noise should be studied through a certain number of trials in order to evaluate the bias (mean value) and the standard deviation.

3.3 Identification with experimental data

From the analysis above, it can be concluded that the result of identification depends on the following factors: the number of estimated parameters and the initial value of parameters for identification. Therefore, choosing an efficient conditions and procedure for the identification is very important. In the next section, the identification is dealt with the data acquired from experiment. The experiment data is separated in 2 sets: first set used for the identification, the second set used for the validation. The process of identification is divided in two steps: First step, all the parameters and the initial states of the INCA robot are estimated. Second step, we estimate the unknown parameters with initial value for identification acquired from the estimated parameters in the first step. The identified model in each step is validated with the validation data set.

3.3.1 Input - Output

The input - output data for the identification are acquired from the experiment with the INCA robot. A software program for providing the currents to the motors and acquiring the data from sensor signal is built based on the real-time Linux framework: 'Xenomai'. It allows to acquire the data with fixed sampling time, in this experiment, the sampling time is 0.01 second. The input signals, introduced in the previous section, are shown in the Figure (3.12). The output signals acquired from the encoders, are presented in the Figure (3.13b). The input sequence and an output sequence are represented as column vectors u and y, respectively, in Matlab. It is suitable to split the data into two sets,

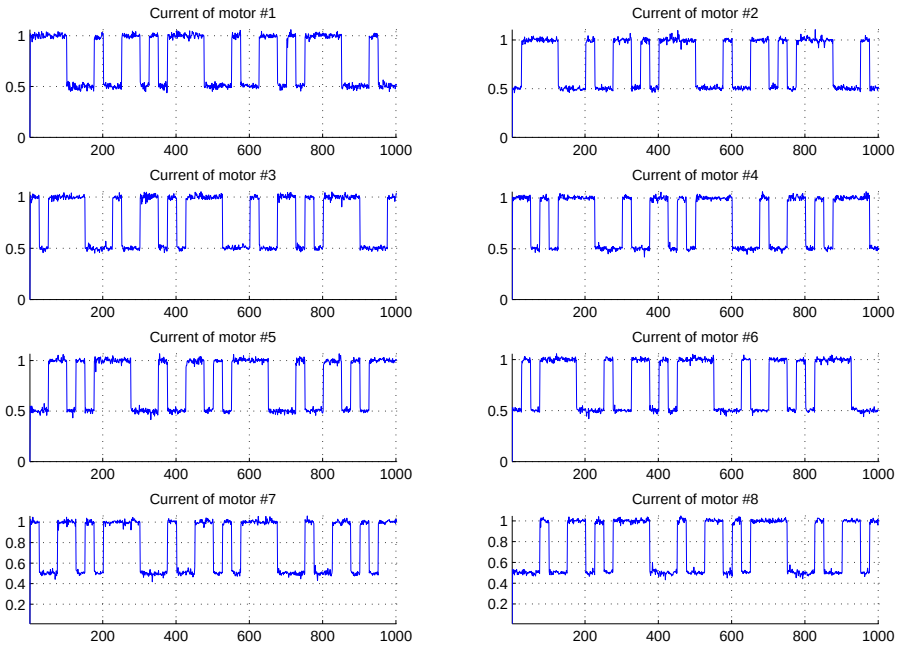

Figure 3.8: *Input signals: Currents of motors*

one for identification and one for validation. Here we use a the first half of the data (from 0 to 5 seconds) to identification, the whole data (from 0 to 10 seconds) is used to validation.

3.3.2 Results

Step.1: Estimate all the parameters

The list of the estimated parameters, obtained in the identification, is shown in Table (3.7). The output: Angle of motor 2, is compared with the measurement data in Figure (3.10). Two values of Loss function are introduced, one presented by Matlab, one computed from Eq. (3.5). The estimated model is validated, Figure (3.11b) presents the comparison between the measurement data and output of the estimated model.

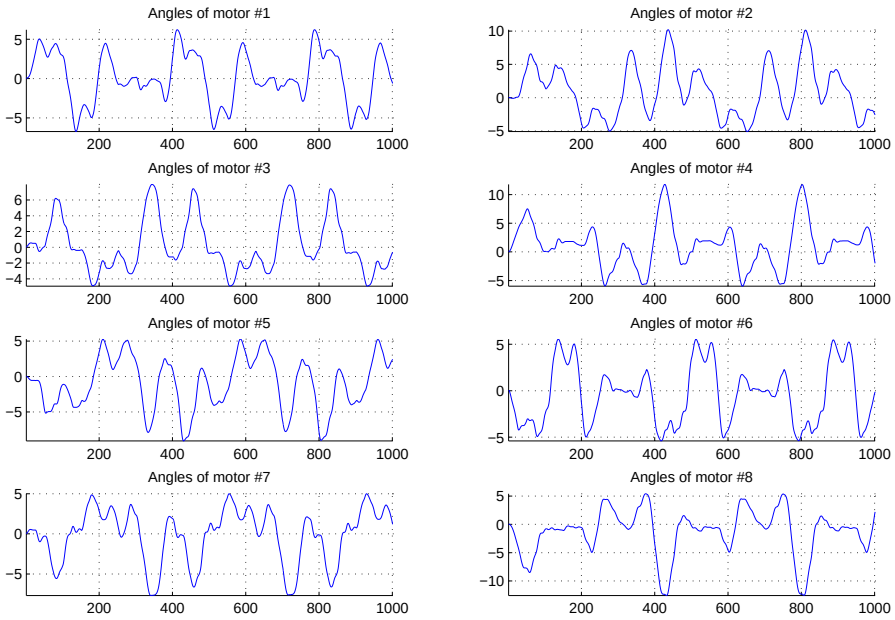

Figure 3.9: *Output signals: Angles of motors*

Parameter	Initial Value	Estimated Value
R (m)	0.0175	0.0148
R_s (m)	0.006	0.0085
k_s (N/m)	16	18.877
λ (N.m/m)	25000	36540.3
b	2	8.107
J (kgm^2)	0.0001	$8.934.10^{-5}$
b_v	0.0002	$7.999.10^{-5}$
b_c	0.005	0.0143
$beta$	0.8	0.9996
K_t (Nm/A)	0.0603	0.1328
m (kg)	0.17246	0.2499
$[x, y, z]_{t=0}$ (m)	$[0, 0, 1.47]$	$[-0.006, -0.005, 1.428]$

Table 3.7: *Step.1: List of estimated parameters*

Step.2: Estimate the unknown parameters

In this subsection, the unknown parameters are estimated. Other parameters which are obtained from the datasheet and from the previous measurement are fixed. The initial

Output	Fitting
Angle of motor 1	87.5%
Angle of motor 2	89.8%
Angle of motor 3	89.3%
Angle of motor 4	89.2%
Angle of motor 5	89.0%
Angle of motor 6	89.1%
Angle of motor 7	89.1%
Angle of motor 8	88.5%
Summary	88.9%
Loss function	6.17686^{-11}
	0.0020

(a) *Estimation: Fitting result of output*

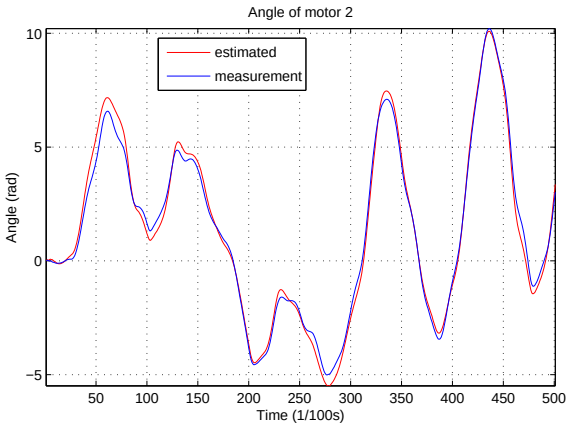

(b) *Estimation: Measurement - estimated angle of motor 2*

Figure 3.10: *Step.1: Comparison between measurement data and estimated model output*

Output	Fitting
Angle of motor 1	87.1%
Angle of motor 2	90.2%
Angle of motor 3	89.8%
Angle of motor 4	89.2%
Angle of motor 5	89.1%
Angle of motor 6	88.2%
Angle of motor 7	89.7%
Angle of motor 8	88.0 %
Summary	88.9%
Loss function	0.0025

(a) *Validation: Fitting result of output*

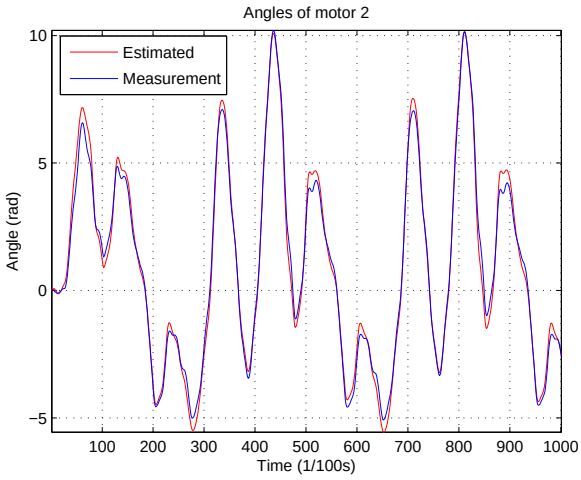

(b) *Validation: Measurement - estimated angle of motor 2*

Figure 3.11: *Step.1: Validation of estimated output*

values for identification of the unknown parameters are obtained from the results of the first step. The list of the estimated parameters, obtained in the identification, is shown in Table (3.8). The output: Angle of motor 2, is compared with the measurement data in Figure (3.10). Two values of Loss function are introduced, one presented by Matlab, one computed from Eq. (3.5). The estimated model is validated, Figure (3.11b) presents the comparison between the measurement data and output of the estimated model.

Parameter	Initial Value	Estimated Value
R (m)	0.0175	0.0115
R_s (m)	0.006	fix
k_s (N/m)	16	fix
λ (N.m/m)	36540.3	26407.7
b	8.107	fix
J (kgm^2)	$8.935.10^{-5}$	$8.342.10^{-5}$
b_v	$7.999.10^{-5}$	$8.366.10^{-5}$
b_c	0.01428	0.01457
$beta$	0.9996	0.9189
K_t (Nm/A)	0.08	0.073
m (kg)	0.25	0.2384
$[x, y, z]_{t=0}$ (m)	$[0, 0, 1.43]$	fix

Table 3.8: *Step.2: List of estimated parameters*

Output	Fitting
Angle of motor 1	87.9%
Angle of motor 2	89.9%
Angle of motor 3	89.9%
Angle of motor 4	88.8%
Angle of motor 5	89.8%
Angle of motor 6	88.5%
Angle of motor 7	89.9%
Angle of motor 8	88.3%
Summary	89.1%
Loss function	9.5359^{-11}
	0.0019

(a) *Estimation: Fitting result of output*

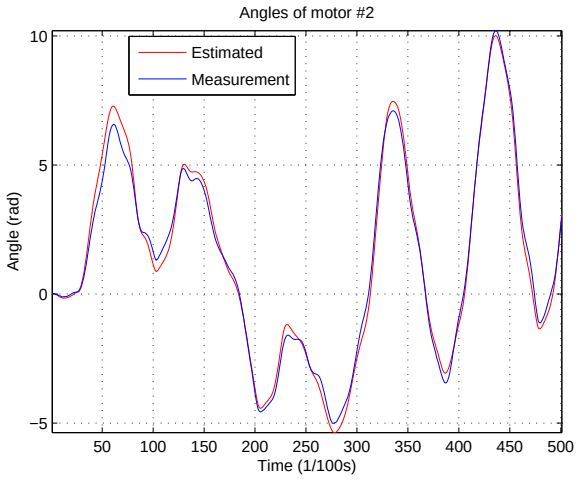

(b) *Estimation: Measurement - estimated angle of motor 2*

Figure 3.12: *Step.1: Comparison between measurement data and estimated model output*

Conclusion

Comparing two experiment results, we can see, the fitting percentages of the output are improved, but very limited. However, the estimated parameters are getting nearer the value written in datasheet or obtained from measurement. The errors could come from the identifiability of each parameter.

Output	Fitting
Angle of motor 1	87.99%
Angle of motor 2	90.9%
Angle of motor 3	90.5%
Angle of motor 4	88.6%
Angle of motor 5	90.2%
Angle of motor 6	88.4%
Angle of motor 7	90.4%
Angle of motor 8	87.9 %
Summary	89.4%
Loss function	0.0022

(a) *Validation: Fitting result of output*

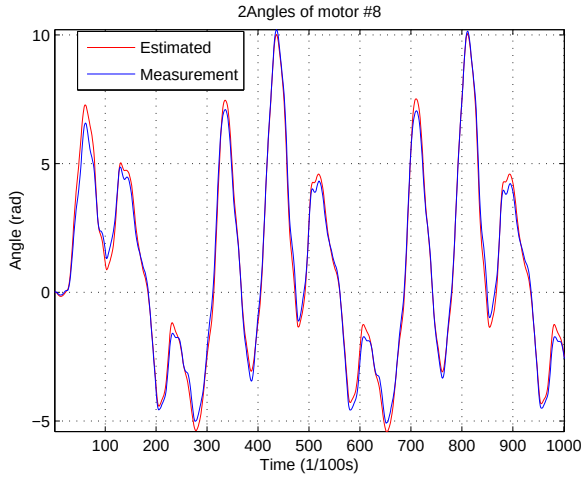

(b) *Validation: Measurement - estimated angle of motor 2*

Figure 3.13: *Step.2: Validation of estimated output*

Chapter 4

Conclusions and future work

Contents

4.1 Summary and Conclusions

In summary, this work aimed to develop the dynamic models of the INCA robot from the laws of physics and to estimate their parameters from the experimental data. To archive this goal, in Chapter 1, the group of Cable Driven Parallel Robots (CDPRs) is introduced, the previous researches in modelling the dynamics of CDPRs are studied in order to decide the most effective method for analysing the dynamics of the INCA robot. Moreover, in Chapter 1, the method 'grey-box' identification are presented. Because of its advantages, it was chosen as method for identification of the INCA robot.

In Chapter 2, the mechanical structure of the INCA robot is introduced, the special dynamic properties are emphasised, thereby the dynamic analysing method is proposed with several assumptions in order to simplify the dynamic model of the INCA robot. Firstly, the kinematics of the INCA robot is investigated by using geometric method in the same way as with the rigid parallel robots. Then, the dynamics of each constituent block of the INCA robot is analysed separately. The elasticity of the cable and its damping behaviour which depend on the action of the roller, are accounted. A nonlinear state-space system, which describes the dynamic model of the INCA robot is obtained.

In Chapter 3, the nonlinear grey-box model is constructed from the state-space functions, received from the previous chapter. In order to provide a more efficient procedure for identification of the INCA robot, several trials of the identification with simulated data are processed. The possible factors, which can affect the identification results, are investigated. Finally, the nonlinear grey-box model of the INCA robot is identified with experimental data, using procedure deducted from the investigation above.

To conclude, the major contributions of this work are:

- the dynamic model for the INCA robot. Furthermore, the technique for modelling dynamics of the INCA robot can be applied to many others flexible robot.
- the estimated grey-box model of the INCA robot. It can be used as a reference for LPV identification of the INCA robot in future.
- the technique for nonlinear grey-box identification from the dynamic model and the experimental data, based on analysing the identification with simulated data.

4.2 Future work

The work presented in this thesis opens up several areas of potential future work in two areas: modelling and identification. In modelling of the INCA robot, the dynamic model of the INCA robot can be developed with the purpose of having the nearest model to the real dynamics of the INCA robot. One possibility is to investigate the effects of the mass of cable on system. When the mass of cable is accounted, in sequence the dynamics of cable must be analysed in dynamics of system. Moreover, the mass of cable with the addition of the elasticity of its make the cable sag. The phenomenon of cable sag will change the static length of cable, and have effects on the tensions of cable. Another possible development is applying the Finite Element Method for the elastic cable.

In identification of the INCA robot, the identification procedure can be developed in order to obtain the 'best' parametric model for the INCA robot. The approach of developing could consist in building better algorithm for searching parameter or improving the grey-box model.

Bibliography

[1] A.B. Alp and S.K. Agrawal, *Cable suspended robots: design, planning and control*, vol. 4, 2002, pp. 4275 – 4280 vol.4. 2

[2] T. Bohlin, *Practical grey-box process identification - theory and applications*, Advances in Industrial Control (2006). 3

[3] Torsten Bohlin, *A case study of grey box identification*, Automatica **30** (1994), no. 2, 307 – 318. 3

[4] Tony Charibon, *Guide de maintenance inca 3d-6d*, Haption S.A. (2009). 4

[5] M. Toti E. Ottaviano, M. Ceccarelli and C.A. Carrasco, *The nist robocrane*, Catrasys (cassino tracking system): A wire system for experimental evaluation of robot workspace **14** (2002), no. 1, 78–87. 2

[6] Paolo Gallina and Robert L. Williams II Aldo Rossi, *Planar cable-direct-driven robots, part ii: Dynamics and control*, ASME Design Engineering Technical Conferences (2001). 3

[7] M. Daemi Grotjahn, M. and B. Heimann, *Friction and rigid body identification of robot dynamics*, International Journal of Solids and Structures **38** (2001), 1889–1902. 3

[8] Albus J., *The nist robocrane*, Int J Robot Syst **10** (1993), no. 5. 2

[9] Kim S. Jeong, J. and Y Kwak, *Kinematics and workspace analysis of a parallel cable mechanism for measuring a robot pose*, Mechanism and Machine Theory **34** (1999), no. 6, 825–841. 3

[10] M. H. Korayem and M. Saadat M. Bamdad, *Workspace analysis of cable-suspended robots with elastic cable*, Proceedings of the 2007 IEEE International Conference on Robotics and Biomimetics (2007), 1942–1947. 3

[11] Qian Zhou Kris Kozak and Jinsong Wang, *Static analysis of cable-driven manipulators with non-negligible cable mass*, IEEE TRANSACTIONS ON ROBOTICS **22** (2006), no. 3. 3

[12] P. Lafourcade and M. Llibre, *Design of a parallel wire-driven manipulator for wind tunnels*, Proceedings of the Workshop on Fundamental Issues and Future Research Directions for Parallel Mechanisms and Manipulators (2002), 187–194. 2

[13] L Ljung, *System identification toolbox user's guide*, (1988). 3

[14] S. Gunnarsson Ostring, M. and M. Norrlof, *Closed-loop identification of an industrial robot containing flexibilities*, Control Engineering Practice **11** (2003), 291–300. 3

[15] Cong Bang Pham, Song Huat Yeo, Guilin Yang, and I-Ming Chen, *Workspace analysis of fully restrained cable-driven manipulators*, Robot. Auton. Syst. **57** (2009), no. 9, 901–912. 2, 3

[16] Makoto Sato, *Development of string-based force display : Spidar*, 8th International conference on virtual systems and multimedia (2001). 4

[17] K. Kurahashi T. Morizono and S. Kawamura, *Realization of a virtual sports training system with parallel wire mechanism*, Proceedings of IEEE Conference on Robotics and Automation (1997), 3025–3030. 2

[18] ShiLiang Dai Yuan Cheng, Gexue Ren, *The multi-body system modelling of the goughstewart platform for vibration control*, J. Sound and Vibration (2004), 599–614. 3